

# Credit Assignment with Resets in Language Model Reasoning

Ankur Samanta<sup>1,2,\*</sup>, Akshayaa Magesh<sup>1</sup>, Ayush Jain<sup>1</sup>, Youliang Yu<sup>1</sup>, Daniel Jiang<sup>1</sup>, Kavosh Asadi<sup>1</sup>, Kaveh Hassani<sup>3</sup>, Paul Sajda<sup>2</sup>, Jalaj Bhandari<sup>1</sup>, Yonathan Efroni<sup>4</sup>

<sup>1</sup>Meta AI, <sup>2</sup>Columbia University, <sup>3</sup>Meta Superintelligence Labs, <sup>4</sup>Tel Aviv University

\*Work done at Meta

Contemporary reinforcement learning with verifiable reward methods post-train language models on multi-step reasoning by assigning a single outcome reward uniformly across all tokens in a trajectory. Such uniform assignment ignores which steps contributed to success or failure. Improving credit assignment can address this limitation by enabling targeted refinement of faulty reasoning steps, rather than updating entire trajectories uniformly. Resets are one such simple mechanism, enabling more precise credit assignment by returning to an intermediate state and resampling counterfactual continuations, so that outcome differences can be attributed to decisions made at that point. We propose two such methods: Random-Reset Policy Optimization (RRPO), where reset states are drawn randomly from reasoning steps, and Self-Reset Policy Optimization (SRPO), where the model self-localizes the erroneous step in an incorrect trajectory and resets there. We analyze these methods within the Conservative Policy Iteration (CPI) framework. Extending CPI with a credit-assignment oracle that targets improvable states yields provable improvements over random resets. Across models and reasoning benchmarks, SRPO consistently outperforms standard GRPO and RRPO by sampling multiple suffix continuations at a self-localized reset and learning from their rewards, using only the model itself with no external supervision.

**Date:** May 27, 2026

**Correspondence:** Ankur Samanta at [as7416@columbia.edu](mailto:as7416@columbia.edu)



## 1 Introduction

Contemporary reinforcement learning with verifiable rewards (RLVR) methods post-train language models by propagating a single outcome reward uniformly across all intermediate steps. For language models on long multi-step reasoning tasks, this assigns identical credit to every step, obscuring which were most responsible for the observed outcome. Learning from steps that most directly shape the outcome can enable efficient learning as it provides a more meaningful signal for policy updates. Such mechanisms are also found in biological systems, which reinstate high-impact decision points and learn from counterfactual “what if” outcomes simulated from those states (Witkowski et al., 2025; Gerstenberg, 2024). Motivated by this, we study RL post-training methods that use resets to improve credit assignment by learning from the counterfactual outcomes of improvable states.

### Credit Assignment with Resets

A reset re-enters a previously-visited state and resamples a continuation, binding outcome differences to the decisions made from that state. In this work, we argue that resets are useful for credit assignment when the reset state admits a strictly better action, namely, when it has significant potential for improvement.

We propose two reset-based RLVR post-training methods for language models, Random-Reset Policy Optimization (RRPO) and Self-Reset Policy Optimization (SRPO). Both resample multiple suffix continuations from a reset state drawn from a failed trajectory, and apply the policy gradient only to those suffix tokens. This shared-prefix group can be thought of as a counterfactual group of rollouts whose outcome differences

attribute credit to the divergent suffix tokens. They differ in how the reset state is chosen. RRPO chooses it uniformly at random across the reasoning steps, while SRPO chooses it via self-localization of the first erroneous step. SRPO requires no external step-level feedback, leveraging Samanta et al. (2026)’s finding that language models can self-localize the first erroneous thought in failed structured-reasoning traces well enough to drive self-correction (see Figure 1).

To quantify the gain over random resets from self-localization of errors, we use the framework of Conservative Policy Iteration (CPI; Kakade and Langford, 2002), a foundational algorithm for policy optimization. CPI draws on-policy state samples via random resets, estimates advantages, and applies a conservative policy update. We refer to this algorithm as CPI-with-random-resets (CPI-RR). We compare its performance to an alternative CPI algorithm that assumes access to a credit-assignment oracle: a membership test for improvable states, answering whether a state admits an action with advantage greater than a threshold  $\tau$ . The resulting variant, CPI-CARO, uses the oracle to draw reset states only from improvable states and applies the policy update only there. We establish that CPI-CARO reduces sample complexity by  $1/p_\pi^2$  and increases per-iteration improvement by  $1/p_\pi$  over CPI-RR, where  $p_\pi$  is the on-policy probability of reaching improvable states.

On a 10-benchmark suite spanning math, science, strategic, and commonsense reasoning, SRPO outperforms GRPO and contemporary RL baselines that use self-correction or shared-prefix continuation. We also test SRPO in a coding domain (LiveCodeBench), where it converges to a higher pass rate and learns 2–3 $\times$  faster than GRPO and RRPO. Higher-quality self-localizations yield higher correction rates and better suffix groups: clean prefixes correct nearly 2 $\times$  as often as erroneous ones, establishing explicit self-localization as an *imperfect but effective* proxy for the credit-assignment oracle. This sensitivity to localization quality motivates further work on improving it in reset-based RL to enable more efficient learning.

### Contributions.

1. *Conceptual.* We frame resets as a credit-assignment primitive for post-training of language models: outcome differences across suffixes resampled from an improvable state bind credit to the decisions made at that state.
2. *Theory.* We extend CPI with a credit-assignment oracle that concentrates resets on states with room to improve, yielding provable improvements over random resets (Theorem 1).
3. *Algorithm and empirical.* We propose SRPO, a post-training RLVR method that resets to a self-localized erroneous step and resamples several alternative continuations, requiring no external step-level supervision. SRPO shows improved performance compared to GRPO. We further provide guidelines for designing reset-based RL methods, and show that self-localization quality drives correction rate and reset-group quality.

## 2 Preliminaries

We study finite-horizon Markov Decision Processes (MDPs) specified by a tuple  $(\mathcal{X}, \mathcal{Y}, P, r, H, \mu)$ , where  $\mathcal{X}$  is the state space,  $\mathcal{Y}$  is the action space,  $H \geq 1$  is the horizon,  $\mu \in \Delta(\mathcal{X})$  is the initial state distribution,  $P = (P_1, \dots, P_H)$  is a sequence of transition kernels  $P_h : \mathcal{X} \times \mathcal{Y} \rightarrow \Delta(\mathcal{X})$ , and  $r = (r_1, \dots, r_H)$  is a sequence of reward functions  $r_h : \mathcal{X} \times \mathcal{Y} \rightarrow \mathbb{R}$ .

A policy  $\pi = (\pi_1, \dots, \pi_H)$  is a sequence of decision rules  $\pi_h : \mathcal{X} \rightarrow \Delta(\mathcal{Y})$ . Executing  $\pi$  from  $x_1 \sim \mu$  induces a trajectory  $(x_1, y_1, \dots, x_H, y_H)$  via  $y_h \sim \pi_h(\cdot | x_h)$  and  $x_{h+1} \sim P_h(\cdot | x_h, y_h)$ , and yields return  $\sum_{h=1}^H r_h(x_h, y_h)$ . The objective is the expected return  $J(\pi) := \mathbb{E}_\pi \left[ \sum_{h=1}^H r_h(x_h, y_h) \right]$ .

For a policy  $\pi$  and time  $h$ , the value function, action-value function, and advantage function are defined for all  $x \in \mathcal{X}$  and  $y \in \mathcal{Y}$  as

$$V_h^\pi(x) := \mathbb{E}_\pi \left[ \sum_{t=h}^H r_t(x_t, y_t) \mid x_h = x \right], \quad Q_h^\pi(x, y) := r_h(x, y) + \mathbb{E}_{x' \sim P_h(\cdot | x, y)} [V_{h+1}^\pi(x')],$$

$$A_h^\pi(x, y) := Q_h^\pi(x, y) - V_h^\pi(x),$$

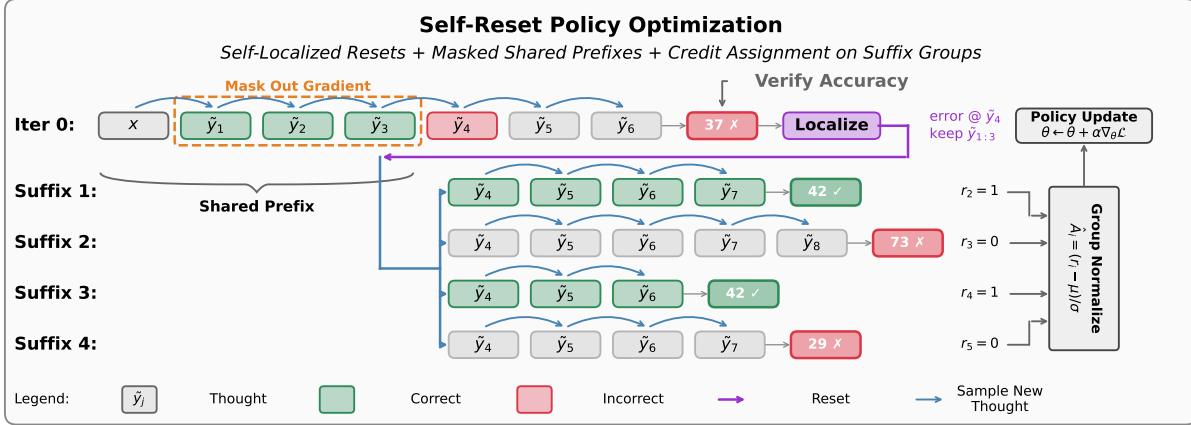


**Figure 1** Self-Reset Policy Optimization (SRPO). The base policy produces an initial rollout (Iter 0) that fails. The model self-localizes the first erroneous thought ( $\tilde{y}_4$ ) and resets to the improvable prefix  $\tilde{y}_{1:3}$ . From this shared prefix, multiple suffix rollouts are sampled, each receiving a reward  $r_i$ . Group normalization converts rewards to advantages  $\hat{A}_i$ , which drive the policy update; the gradient on the shared prefix is masked out so the update is concentrated on the suffix tokens.

with the convention  $V_{H+1}^\pi \equiv 0$ . The time- $h$  state distribution under  $\pi$  is  $d_\pi^h(x) := \mathbb{P}_\pi(x_h = x \mid x_1 \sim \mu)$  for all  $x \in \mathcal{X}$ , and the time-averaged state distribution is  $d_{\pi, \mu}(x) := \frac{1}{H} \sum_{h=1}^H d_\pi^h(x)$  for all  $x \in \mathcal{X}$ .

The *greedy policy* with respect to  $\pi$  is the sequence  $\pi^+ = (\pi_1^+, \dots, \pi_H^+)$  with  $\pi_h^+(x) := \arg \max_{y \in \mathcal{Y}} A_h^\pi(x, y)$  for all  $x \in \mathcal{X}$ . For any policy  $\pi'$ , the *policy advantage* of  $\pi'$  against  $\pi$  is  $\mathbb{A}_{\pi, \mu}(\pi') := \frac{1}{H} \sum_{h=1}^H \mathbb{E}_{x \sim d_\pi^h} \mathbb{E}_{y \sim \pi'_h(\cdot | x)} [A_h^\pi(x, y)]$ .

### 3 From Random to Credit-Assignment Based Resets in CPI

Conservative Policy Iteration (CPI; [Kakade and Langford, 2002](#)) is a foundational algorithm for approximate policy improvement, with provably monotone-improvement guarantees. CPI’s framework underlies TRPO ([Schulman et al., 2015](#)), PPO ([Schulman et al., 2017](#)), MDPO ([Tomar et al., 2020](#)), and GRPO ([Shao et al., 2024](#)), which are commonly used in modern language model post-training. Each CPI update can be interpreted as a small gradient step on the policy, a Frank-Wolfe ([Frank and Wolfe, 1956](#)) update on  $J(\pi)$  ([Vieillard et al., 2020](#); [Sherman et al., 2025](#)). We refer to this procedure as CPI-RR.

CPI improves a policy  $\pi$  by *random-reset sampling*: draw  $x \sim d_\pi^h$  at a uniformly-random time  $h$ , take a random action  $y \sim \text{Unif}(\mathcal{Y})$ , and roll out  $\pi$  to the horizon to obtain an unbiased estimate of  $Q_h^\pi(x, y)$ . Aggregating these estimates fits  $A_h^\pi$  and yields the greedy update direction  $\pi^+$ .  $\pi$  is then updated via the conservative mixture  $\pi_\alpha = (1 - \alpha)\pi + \alpha\pi^+$ ; for a suitable step size  $\alpha$ , CPI guarantees monotone improvement at a rate governed by the policy advantage  $\mathbb{A}_{\pi, \mu}(\pi^+)$ .

A closer look reveals that the improvement magnitude is governed by states with a specific property.  $\mathbb{A}_{\pi, \mu}(\pi^+)$ , an expectation of  $\pi^+$ ’s advantage over  $\pi$  under on-policy visitation, is dominated by *large-advantage states* where  $\pi$  admits a strictly better action. Random-reset sampling draws uniformly from  $d_{\pi, \mu}$ , diluting this signal rather than concentrating it where the gain lives. Modern language models can target such states directly. Given a failed reasoning trajectory, they self-localize the erroneous thought, precisely a state where a different action would have changed the outcome ([Yang et al., 2026b](#); [Samanta et al., 2026](#)). We abstract this capability as a *credit-assignment oracle* and study the resulting CPI variant, CPI-CARO, in the next subsection. Table 1 previews its provably better sample complexity and per-iteration improvement over CPI-RR.

**Table 1** Sample complexity and per-iteration improvement for CPI-RR and CPI-CARO in the regime  $\mathbb{A}_{\pi,\mu}^{\mathcal{G}^c}(\pi^+) \ll \tau$ . CPI-CARO saves a  $p_\pi^2$  factor in sample complexity and gains a  $1/p_\pi$  factor in per-iteration improvement. In the RLVR setting studied in Section 4, we define a state as improvable if an error was made during its reasoning trace. Under this definition,  $\mathbb{A}_{\pi,\mu}^{\mathcal{G}^c}(\pi^+) = 0$ : if no error was made, the agent outputs the correct solution and there is no opportunity to improve upon it. See Theorem 1 and Section 3.2.

	Samples	Per-iteration improvement
CPI-RR	$\tilde{O}\left(\frac{ \mathcal{Y}  H^2 R_{\max}^2}{\tau^2 p_\pi^2}\right)$	$\Omega\left(\frac{\tau^2 p_\pi^2}{H R_{\max}}\right)$
CPI-CARO	$\tilde{O}\left(\frac{ \mathcal{Y}  H^2 R_{\max}^2}{\tau^2}\right)$	$\Omega\left(\frac{\tau^2 p_\pi}{H R_{\max}}\right)$

### 3.1 CPI with a Credit-Assignment Reset Oracle

We now formalize the credit-assignment oracle and analyze the CPI variant that uses it.

*Formalizing the Credit-Assignment Reset Oracle.* Fix a threshold  $\tau > 0$ . For each  $h \in [H]$ , the  $\tau$ -improvable set at time  $h$  is  $\mathcal{G}_{h,\tau} := \{x \in \mathcal{X} : \max_{y \in \mathcal{Y}} A_h^\pi(x, y) \geq \tau\}$ . Let  $p_{\pi,h} := \mathbb{P}_{x \sim d_\pi^h}[x \in \mathcal{G}_{h,\tau}]$  denote the time- $h$  coverage of  $\mathcal{G}_{h,\tau}$ , and let the coverage of  $\pi$  at threshold  $\tau$  be the time-averaged quantity  $p_\pi := \frac{1}{H} \sum_{h=1}^H p_{\pi,h}$ . We assume  $p_\pi > 0$  throughout this section. If  $p_\pi = 0$  then  $\pi_{\mathcal{G}} \equiv \pi$  and the algorithm makes no update. The credit-assignment greedy policy plays  $\pi^+$  on the improvable set and  $\pi$  elsewhere: for all  $h \in [H]$ ,  $x \in \mathcal{X}$ ,  $y \in \mathcal{Y}$ ,

$$(\pi_{\mathcal{G}})_h(y | x) := \begin{cases} \pi_h^+(y | x) & \text{if } x \in \mathcal{G}_{h,\tau}, \\ \pi_h(y | x) & \text{otherwise.} \end{cases}$$

A credit-assignment oracle is a membership test  $\mathcal{O}(x, h) = \mathbf{1}\{x \in \mathcal{G}_{h,\tau}\}$ , and the corresponding credit sampler  $\text{CREDIT\_SAMPLER}(\pi, \mu)$  returns pairs  $(x, h)$  with  $h \sim \text{Unif}[H]$ ,  $x \sim d_\pi^h$ , conditioned on  $x \in \mathcal{G}_{h,\tau}$ . Finally, for any policy  $\pi'$ , the conditional policy advantages on and off  $\mathcal{G}_{h,\tau}$  are  $\mathbb{A}_{\pi,\mu}^{\mathcal{G}}(\pi') := \mathbb{E}[A_h^\pi(x, y) | x \in \mathcal{G}_{h,\tau}]$  and  $\mathbb{A}_{\pi,\mu}^{\mathcal{G}^c}(\pi') := \mathbb{E}[A_h^\pi(x, y) | x \notin \mathcal{G}_{h,\tau}]$ , with expectations taken under  $h \sim \text{Unif}[H]$ ,  $x \sim d_\pi^h$ ,  $y \sim \pi'_h(\cdot | x)$ .

Since  $\pi_{\mathcal{G}}$  deviates from  $\pi$  only on  $\mathcal{G}_{h,\tau}$ , its policy advantage simplifies to  $\mathbb{A}_{\pi,\mu}(\pi_{\mathcal{G}}) = p_\pi \mathbb{A}_{\pi,\mu}^{\mathcal{G}}(\pi^+) \geq \tau p_\pi$ . Knowing the membership in  $\mathcal{G}_{h,\tau}$ , the credit sampler estimates this conditional advantage  $\mathbb{A}_{\pi,\mu}^{\mathcal{G}}(\pi^+) \geq \tau$  directly, a  $1/p_\pi$ -larger signal than the diluted  $\mathbb{A}_{\pi,\mu}(\pi^+) \geq \tau p_\pi$  that random-reset sampling targets. This motivates a CPI variant designed around the oracle, which we describe next.

*Algorithms.* We adapt CPI-RR into CPI-CARO, a variant that uses the credit sampler to target states with large potential improvement. Algorithm 1 presents both in a single block. CPI-CARO differs from CPI-RR in exactly two steps: it samples  $(x, h)$  from the credit sampler rather than the on-policy distribution, and applies the conservative update only on  $\mathcal{G}_{h,\tau}$ .

*Implementing the sampler.* Given the credit-assignment oracle  $\mathcal{O}$ , the credit sampler is implemented via rejection sampling: draw  $(x, h)$  from the on-policy distribution, accept if  $\mathcal{O}(x, h) = 1$ , reject otherwise. This costs  $O(n/p_\pi)$  cheap queries for  $n$  accepted samples, with expensive Q-rollouts run only on accepted draws. We defer the formal procedure to Appendix B.

*Main guarantee.* Theorem 1 quantifies the sample complexity and per-iteration improvement of both variants (see Appendix A.2 for the proof).

**Theorem 1** (Sample complexity and per-iteration improvement). *Assume the function class  $\mathcal{F}$  is finite and realizable, namely,  $Q_h^\pi \in \mathcal{F}$  and rewards are bounded in  $r_h \in [0, R_{\max}]$  for all  $h \in [H]$ . Fix  $\delta \in (0, 1)$  and define  $N_0 := C |\mathcal{Y}| H^2 R_{\max}^2 \log(|\mathcal{F}|/\delta)$  for some constant  $C > 0$ . With probability at least  $1 - \delta$ , Algorithm 1 returns a policy  $\pi_{\hat{\alpha}}$  satisfying:*

---

**Algorithm 1** CPI-RR / CPI-CARO
 

---

**Require:** policy  $\pi$ , function class  $\mathcal{F}$ , threshold  $\tau$ , sample size  $n$

```

// Phase 1: Q-sampling
1: for  $i = 1, \dots, n$  do
2:    $(x_i, h_i) \leftarrow \text{SAMPLER}(\pi, \mu)$  ▷ on-policy draw
3:    $(x_i, h_i) \leftarrow \text{CREDIT SAMPLER}(\pi, \mu)$  ▷ draw conditioned on  $\mathcal{G}_{h,\tau}$ 
4:   sample  $y_i \sim \text{Unif}(\mathcal{Y})$ 
5:    $\hat{Q}_i \leftarrow \text{QROLLOUT}(\pi, x_i, y_i, h_i)$ 
6: end for
// Phase 2: fit, derive greedy, estimate advantage
7:  $\hat{Q} \leftarrow \arg \min_{f \in \mathcal{F}} \sum_{i=1}^n (f(x_i, y_i, h_i) - \hat{Q}_i)^2$ 
8:  $\hat{\pi}_h^+(x) \leftarrow \arg \max_{y \in \mathcal{Y}} \hat{Q}(x, y, h)$ 
9:  $\hat{\mathbb{A}} \leftarrow \frac{1}{n} \sum_{i=1}^n |\mathcal{Y}| (\hat{\pi}_{h_i}^+(y_i | x_i) - \pi_{h_i}(y_i | x_i)) \hat{Q}(x_i, y_i, h_i)$ 
// Phase 3: conservative update
10:  $\hat{\alpha} \leftarrow \min\{1, \hat{\mathbb{A}} / (H^2 R_{\max})\}$  ▷ step from Kakade and Langford (2002)
11:  $\hat{\alpha} \leftarrow \min\{1, \hat{\mathbb{A}} / (2 H^2 R_{\max})\}$  ▷ step from Cor. 5 (Appendix A.1)
12: return  $\pi_{\hat{\alpha}} \leftarrow (1 - \hat{\alpha}) \pi + \hat{\alpha} \hat{\pi}^+$  on all states
13: return  $\pi_{\hat{\alpha}} \leftarrow (1 - \hat{\alpha}) \pi + \hat{\alpha} \hat{\pi}^+$  on  $\mathcal{G}_{h,\tau}$ ;  $\pi$  on  $\mathcal{G}_{h,\tau}^c$ 

```

---

a) *CPI-RR.* With sample size  $n \geq \frac{N_0}{\tau^2 p_\pi^2}$ , it holds that

$$J(\pi_{\hat{\alpha}}) - J(\pi) \geq \frac{\mathbb{A}_{\pi,\mu}(\pi^+)^2}{8 H R_{\max}} \geq \frac{\tau^2 p_\pi^2}{8 H R_{\max}},$$

where the second inequality is tight in the regime  $\mathbb{A}_{\pi,\mu}^{\mathcal{G}}(\pi^+) \ll \tau$ .

b) *CPI-CARO.* With sample size  $n \geq \frac{N_0}{\tau^2}$ , it holds that

$$J(\pi_{\hat{\alpha}}) - J(\pi) \geq \frac{\tau^2 p_\pi}{16 H R_{\max}}.$$

The gain is most pronounced when  $p_\pi$  is small, exactly the regime where the probability to hit a state in the improvable set is small and CPI-RR spends most of its budget on states without signal. The improvement of CPI-CARO over CPI-RR is largest when  $\mathbb{A}_{\pi,\mu}^{\mathcal{G}}(\pi^+) \ll \tau$ , in which case  $\mathbb{A}_{\pi,\mu}(\pi^+) \sim p_\pi \mathbb{A}_{\pi,\mu}^{\mathcal{G}}(\pi^+) \geq p_\pi \tau$  (see Lemma 2). Next, we explain the mechanism behind both improvements.

### 3.2 Where Does the Improvement Come From?

CPI is built around the lower bound (Kakade and Langford, 2002):

$$J(\pi_\alpha) - J(\pi) \geq \alpha H \mathbb{A}_{\pi,\mu}(\pi^+) - \frac{1}{2} \alpha^2 H^3 R_{\max}. \quad (1)$$

Maximizing the right-hand side on  $\alpha$  recovers the step  $\alpha^* \propto \mathbb{A}_{\pi,\mu}(\pi^+) / (H^2 R_{\max}) \sim \tau p_\pi / (H^2 R_{\max})$  assuming that the advantage of  $\pi^+$  on states not in  $\mathcal{G}$  is vanishing, namely  $\mathbb{A}_{\pi,\mu}^{\mathcal{G}^c}(\pi') \ll \tau$ . Both scale with the lower bound on the policy advantage that the algorithm can guarantee. Without oracle access, the only lower bound on  $\mathbb{A}_{\pi,\mu}(\pi^+)$  derivable from  $\tau$  and  $p_\pi$  is  $\tau p_\pi$ . Estimating this minimum guaranteed advantage requires  $n \gtrsim |\mathcal{Y}| H^2 R_{\max}^2 / (\tau^2 p_\pi^2)$  samples, matching CPI-RR's rate in Theorem 1 and shown tight via a finite-sample Cramer bound (see Appendix A.3).

For CPI-CARO, the update applies  $\pi^+$  only on  $\mathcal{G}_{h,\tau}$ . This restriction yields a credit-aware simulation lemma and the following credit-aware CPI lower bound (see Appendix A.1),

$$J(\pi_\alpha) - J(\pi) \geq \alpha H p_\pi \mathbb{A}_{\pi,\mu}^{\mathcal{G}}(\pi^+) - \alpha^2 H^3 R_{\max} p_\pi. \quad (2)$$

Maximizing the right-hand side now requires estimating  $\mathbb{A}_{\pi,\mu}^{\mathcal{G}}(\pi^+) \geq \tau$ , a  $1/p_\pi$ -larger target. The improvement therefore comes from two effects, acting on different parts of CPI-CARO. The credit-aware simulation lemma

allows a  $1/p_\pi$ -larger step size  $\hat{\alpha} \propto \mathbb{A}_{\pi, \mu}^{\mathcal{G}}(\pi^+) / (H^2 R_{\max}) \sim \tau / (H^2 R_{\max})$ , yielding  $1/p_\pi$  more improvement per iteration. Further, the larger estimation target reduces the sample budget  $n$  at a given precision by  $1/p_\pi^2$ . Together they yield the rate for CPI-CARO as shown in Theorem 1.

## 4 Methods

We translate the theory of Section 3 into a practical post-training RLVR method through three choices: the granularity of credit assignment (Section 4.1), how to reach and resample from improvable states (Section 4.2), and how to reinforce the rollouts (Section 4.3).

### 4.1 Granularity of Credit Assignment

Our methods use a *thought-level* abstraction, where each action is a semantically coherent reasoning step the model emits as it generates its completion. Other granularities used in prior work include human- or judge-annotated step boundaries (Lightman et al., 2023; Uesato et al., 2022; Wang et al., 2023; Luo et al., 2024), fixed-length token blocks (Wang et al., 2026), and heuristic entropy- or token-count-based segments (Guo et al., 2025). Token-level actions are too fine for sparse-reward credit assignment, while these higher-level abstractions impose boundaries the model itself did not choose, risking incomplete segments. For credit assignment with resets, self-determining each thought’s boundaries during generation makes every thought an atomic, self-contained unit, requiring no retroactive parsing. Importantly, Samanta et al. (2026) shows that language models can reliably localize erroneous thought steps within such structured reasoning traces, making self-localized resets feasible.

We formalize the thought-level generation process as a *Thought MDP*. The initial state  $x_0 \sim \mu$  is the prompt. At step  $h$ , the model emits a thought  $\tilde{y}_h \sim \pi_h(\cdot \mid x_0, \tilde{y}_{1:h-1})$  — a sequence of tokens delimited by a stop pattern — and the prefix  $(x_0, \tilde{y}_{1:h-1})$  fully describes the state. Reward is sparse:  $r_h = 0$  for  $h < H$ , with terminal  $r_H \in \{0, 1\}$  from oracle verification of final-answer correctness.

This granularity has two practical payoffs. First, since the thought structure is induced by prompting alone (rollout prompt in Appendix D), resetting to any prefix state and resampling the next thought when generating rollouts introduces no distributional shift — a precondition for the on-policy reset-and-resample procedure of Section 4.2. Second, the improvable set  $\mathcal{G}_{h, \tau}$  consists of recoverable reasoning errors rather than arbitrary token positions, giving self-localization a meaningful target.

### 4.2 Generating Rollouts by Resetting and Resampling

This section describes how RRPO and SRPO construct training rollouts. Both realize their theoretical counterparts at the thought level: RRPO corresponds to CPI-RR, and SRPO corresponds to CPI-CARO in the RLVR setting, with self-localization of the first erroneous step standing in for the credit-assignment oracle.

At each training step, we build a buffer that combines a base group of  $G$  iid rollouts from the prompt  $x_0$  under standard GRPO with a shared-prefix group of  $G$  rollouts from a reset state  $x^*$  (see Algorithm 2). To construct the shared-prefix group, we draw iid rollouts from  $\pi_\theta(\cdot \mid x_0)$  until the first incorrect one, the *seed* of length  $H_s$  thoughts, then pick a reset index  $h^*$ , form  $x^* = (x_0, \tilde{y}_{1:h^*-1})$ , and sample  $G$  iid thought-level rollouts from  $x^*$ . The seed is excluded from the base group to preserve iid sampling. The two methods differ only in how  $h^*$  is chosen. Figure 2 illustrates the resulting rollout buffer alongside the GRPO baseline and two alternative splits,  $2 \times 4$  and  $1 \times 8$ , studied in Section 5.1. If sampling exhausts without an incorrect rollout, which is rare in practice, the step falls back to standard GRPO on the base group.

*RRPO: random reset.* RRPO draws  $h^* \sim \text{Unif}\{1, \dots, H_s\}$ , so the reset state  $x^*$  is an arbitrary thought-level prefix of the failed seed. This realizes CPI-RR’s uniform reset at the thought level.

*SRPO: self-localized reset.* SRPO sets  $h^*$  via error localization. The localization signal could come from a PRM, step-level environment feedback, or a separate localizer. To avoid auxiliary supervision, we instantiate it with explicit self-localization, where the same policy  $\pi_\theta$  that generated the seed is prompted to analyze its

own reasoning trace. The seed is presented as the labeled sequence of thoughts  $\tilde{y}_1, \dots, \tilde{y}_{H_s}$ , and the model returns the index of the first incorrect thought (see localization prompt in Appendix D). The reset state  $x^*$  is then the self-determined verified-correct prefix preceding that error. This realizes CPI-CARO at the thought level, with the localizer taking the place of the rejection-sampling draw from  $\mathcal{G}_{h,\tau}$  in Algorithm 3.

---

**Algorithm 2** RRPO / SRPO

---

**Require:** prompt  $x_0$ , policy  $\pi_\theta$ , group size  $G$

// Phase 1: base group (on-policy)

- 1: sample iid rollouts from  $x_0$  until the first incorrect one; let it be the *seed*, with thoughts  $\tilde{y}_1, \dots, \tilde{y}_{H_s}$
- 2: collect all preceding correct rollouts as initial members of group 1; discard the seed
- 3: sample additional iid rollouts from  $x_0$  until  $|\text{group 1}| = G$

// Phase 2: shared-prefix group at reset state  $x^*$

- 4:  $h^* \sim \text{Unif}\{1, \dots, H_s\}$  ▷ random reset
- 5:  $h^* \leftarrow$  self-localized index of the seed’s first erroneous thought ▷ oracle reset
- 6:  $x^* \leftarrow (x_0, \tilde{y}_{1:h^*-1})$
- 7: sample  $G$  iid rollouts from  $x^* \rightarrow$  group 2

// Phase 3: advantage estimation (group-normalized within each group)

- 8: **for** each group  $k \in \{1, 2\}$  **do**
- 9:  $\hat{A}_i \leftarrow (r_i - \text{mean}(\mathbf{r}_k)) / \text{std}(\mathbf{r}_k)$  for each rollout  $i$  in group  $k$
- 10: **end for**

// Phase 4: update

- 11: optimize GRPO loss over all  $2G$  rollouts with advantages  $\hat{A}$ ; mask the prefix tokens of  $x^*$  in group 2

---

### 4.3 Reinforcing Rollouts via Group-Relative Advantages

With the two-group rollout buffer assembled, we now turn to the policy update. We learn from each rollout group via group-relative normalization (Shao et al., 2024). For a group of  $G$  rollouts with outcome rewards  $r_1, \dots, r_G$ , rollout  $i$  receives the self-normalized advantage  $\hat{A}_i = (r_i - \mu) / \sigma$ , where  $\mu$  and  $\sigma$  are the group’s empirical mean and standard deviation; each  $\hat{A}_i$  measures rollout  $i$ ’s outcome relative to the rest of its group. With rollouts sampled from the prompt  $x_0$  under standard GRPO, this advantage is broadcast uniformly across every token in the rollout.

For the shared-prefix group, each rollout’s suffix is a token sequence  $y_{i,1}, \dots, y_{i,T_i}$  of length  $T_i$  sampled from  $\pi_\theta(\cdot | x^*)$  to termination, where  $x^* = (x_0, \tilde{y}_{1:h^*-1})$  is the reset state. We mask the shared prefix and apply the group-relative advantage only to suffix tokens, giving the shared-prefix loss  $\mathcal{L}_{\text{SP}}(\theta) = -\frac{1}{G} \sum_{i=1}^G \frac{1}{T_i} \sum_{t=1}^{T_i} \hat{A}_i \log \pi_\theta(y_{i,t} | x^*, y_{i,<t})$ . This prefix masking is the parametric analog of CPI-CARO’s policy update on the reset state. Because  $x^*$  is itself a thought-level prefix, the resulting credit signal lives on thoughts rather than tokens. The base group uses the analogous loss over full rollouts. We take one on-policy gradient step per group, without PPO clipping or KL regularization (Appendix C, Table 4 shows that adding PPO clipping does not help).

## 5 Results

We train Qwen2.5-14B-Instruct (Yang et al., 2024) and OLMo-3-7B-Instruct (Olmo et al., 2025) on NuminaMath-Olympiads (LI et al., 2024) using 400 problems and 2 epochs, and thoroughly test general reasoning performance over a suite of 10 benchmark tasks covering math, science, and strategic reasoning: NuminaMath-Olympiads (LI et al., 2024), HMMT Nov 2025 (Tournament, 2025), MATH Level-5 (Hendrycks et al., 2021), StrategyQA (Geva et al., 2021), AceReason-Math (Liu et al., 2025), SciKnowEval Chemistry (Feng et al., 2024), SciKnowEval Biology (Feng et al., 2024), CommonsenseQA (Talmor et al., 2019), SciKnowEval Materials (Feng et al., 2024), and SciKnowEval Physics (Feng et al., 2024). For each benchmark we evaluate on 500 randomly selected test items. We aggregate all results over 3 seeds; tables report mean  $\pm$  SD with the best per column in bold. Numbers represent final performance after 2 epochs of training. Evaluation uses temperature 0. Each method is roughly compute-matched to result in 8 rollouts per prompt. We train all methods with LoRA adapters (Hu et al., 2021) of rank 64 and  $\alpha = 64$ . Further training details are in Appendix C.

## 5.1 Evaluating Reset-Based Sampling Strategies

We first study how to effectively utilize resets under a fixed compute budget. Holding total compute fixed at 8 rollouts per prompt, we compare three SRPO instantiations (Figure 2):  $1\times 4$  splits the budget as 4 iid base rollouts plus 4 suffixes resampled from one self-localized prefix;  $2\times 4$  doubles prefix diversity (two prefixes, 4 suffixes each) at the cost of the base group;  $1\times 8$  maximizes suffix depth from a single localization.

**Table 2** Sampling-strategy comparison for SRPO under a fixed 8-rollout-per-prompt budget on OLMo-3-7B-Instruct. Full results including Qwen2.5-14B-Instruct in Appendix F.

Method	oly	hmmt	lvl5	stra	ace	chem	bio	csqa	mat	phys
SRPO ( $1\times 4$ )	24.8 $\pm$ 1.9	<b>15.6 <math>\pm</math> 4.2</b>	<b>67.5 <math>\pm</math> 3.5</b>	<b>66.6 <math>\pm</math> 2.5</b>	<b>59.6 <math>\pm</math> 2.6</b>	<b>24.7 <math>\pm</math> 1.4</b>	28.7 $\pm$ 0.6	<b>74.8 <math>\pm</math> 1.0</b>	<b>55.9 <math>\pm</math> 0.6</b>	<b>54.5 <math>\pm</math> 2.0</b>
SRPO ( $2\times 4$ )	<b>26.1 <math>\pm</math> 1.2</b>	14.4 $\pm$ 3.1	66.0 $\pm$ 3.1	65.9 $\pm$ 2.2	56.7 $\pm$ 2.7	22.4 $\pm$ 0.5	27.9 $\pm$ 0.2	65.9 $\pm$ 3.3	45.7 $\pm$ 1.3	43.2 $\pm$ 5.7
SRPO ( $1\times 8$ )	23.1 $\pm$ 2.6	12.2 $\pm$ 3.1	62.3 $\pm$ 2.5	64.1 $\pm$ 3.4	53.7 $\pm$ 6.3	22.8 $\pm$ 1.2	<b>29.8 <math>\pm</math> 1.9</b>	59.5 $\pm$ 14.9	43.5 $\pm$ 5.8	43.4 $\pm$ 8.6

The  $1\times 4$  split wins on the majority of columns, balancing base-policy coverage with shared-prefix depth; the same pattern holds for Qwen2.5-14B-Instruct (Appendix F). We adopt  $1\times 4$  as the default SRPO configuration for the remaining experiments.

## 5.2 General Reasoning Performance

We next compare SRPO and RRPO against GRPO and related baselines (App. 6) in Tab. 3. SRPO is the strongest non-baseline method on both base models, with the best result on 7/10 tasks for Qwen2.5-14B and 6/10 for OLMo-3-7B. Since training uses NuminaMath-Olympiads alone, the gains on the other 9 benchmarks (science, strategic, commonsense, and other math tasks) reflect out-of-distribution generalization. RRPO is comparable to GRPO.

## 5.3 Self-Guided Resets in Coding Tasks

We extend SRPO to coding on LiveCodeBench (Jain et al., 2024) v6 medium (383 problems), holding the problem set fixed across training and evaluation and splitting the per-problem unit tests: a subset is used as the training-time verifier (reward = fraction of train-split test cases passed), and the remainder are held out for evaluation. We train for 1 epoch and compare SRPO, RRPO, and GRPO under a fixed 8-rollout-per-prompt budget (Figure 3). SRPO’s prefix mask concentrates each shared-prefix rollout’s gradient signal onto its suffix tokens, the tokens that distinguish a correction from the failed seed. We measure this signal per token as the gradient magnitude with respect to the sampled token’s logit,  $g_{i,t} = (|\hat{A}_i|/T_i)(1 - \pi_\theta(y_{i,t} | \cdot))$ , where  $T_i$  is the rollout’s active-token count: suffix length for shared-prefix, full response length for base (derivation in Appendix G). Figure 3 colors each thought block by the mean of  $g_{i,t}$  over its active tokens on one SRPO update applied to a LiveCodeBench-medium prompt; shared-prefix rollouts (top) deliver more per-token signal than base rollouts (bottom). Appendix G confirms this throughout training: on prompts where both groups deliver gradient (some rollout has nonzero advantage in each), shared-prefix rollouts receive higher per-token signal at 10 of the 11 training steps. The fraction of prompts where both groups deliver gradient grows throughout training as the model gets better at self-correction: each shared-prefix rollout is conditioned on a failed seed trajectory, so the shared-prefix group starts with lower pass rates than the base group, but as

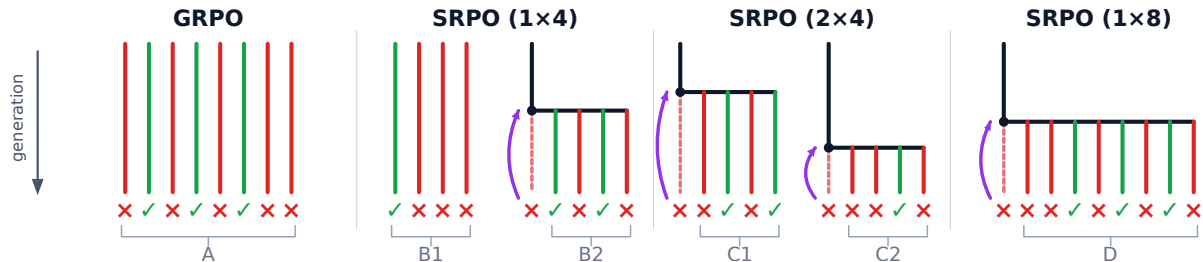


**Figure 2** Reset-based sampling strategies under a fixed 8-rollout-per-prompt budget.

**Table 3** General reasoning performance across math, science, strategic, and commonsense benchmarks.

Method	oly	hmmt	lv15	stra	ace	chem	bio	csqa	mat	phys
<i>Qwen2.5-14B-Instruct</i>										
Base <sup>†</sup>	26.0	6.7	51.0	71.4	44.2	23.6	30.0	65.8	30.0	26.6
GRPO	25.0 ± 1.5	5.6 ± 1.6	52.1 ± 1.2	69.5 ± 2.8	45.2 ± 2.0	<b>26.5 ± 2.2</b>	30.1 ± 1.1	66.1 ± 16.7	29.4 ± 5.7	26.9 ± 6.8
S-CoRe	25.3 ± 1.1	5.6 ± 1.6	54.1 ± 0.5	72.0 ± 0.5	43.7 ± 2.1	25.0 ± 3.2	30.2 ± 1.9	78.0 ± 1.7	30.9 ± 2.3	29.5 ± 4.1
Cr-GRPO	24.9 ± 0.7	<b>7.8 ± 1.6</b>	51.1 ± 0.2	72.1 ± 0.4	42.5 ± 1.2	22.9 ± 0.5	30.9 ± 1.2	66.8 ± 0.7	29.8 ± 1.4	24.9 ± 1.2
SPO-Tree	25.1 ± 1.1	4.4 ± 4.2	51.5 ± 1.2	71.7 ± 1.2	43.1 ± 0.4	23.4 ± 0.9	31.4 ± 0.9	66.7 ± 0.9	29.0 ± 0.2	24.5 ± 1.1
RRPO	<b>25.7 ± 0.9</b>	<b>7.8 ± 1.6</b>	52.7 ± 1.2	69.6 ± 3.9	45.7 ± 2.0	25.6 ± 5.0	33.1 ± 3.7	77.7 ± 2.3	37.5 ± 2.9	39.8 ± 13.0
SRPO	25.5 ± 1.2	6.7 ± 2.7	<b>55.2 ± 0.7</b>	<b>74.9 ± 0.2</b>	<b>46.2 ± 0.9</b>	24.5 ± 3.8	<b>33.9 ± 2.3</b>	<b>80.6 ± 0.9</b>	<b>39.3 ± 2.6</b>	<b>45.5 ± 11.8</b>
<i>OLMo-3-7B-Instruct</i>										
Base <sup>†</sup>	23.2	10.0	56.8	55.0	48.4	19.8	25.8	72.2	44.6	45.4
GRPO	<b>26.6 ± 0.2</b>	11.1 ± 5.7	67.1 ± 1.2	62.0 ± 4.6	<b>59.7 ± 0.8</b>	20.7 ± 0.4	26.3 ± 2.1	72.3 ± 0.6	51.3 ± 2.6	42.3 ± 5.4
S-CoRe	17.3 ± 1.5	0.0 ± 0.0	43.4 ± 6.9	60.2 ± 2.8	33.9 ± 4.2	18.9 ± 1.1	<b>29.6 ± 3.7</b>	71.5 ± 1.1	32.6 ± 5.9	29.4 ± 3.8
Cr-GRPO	21.9 ± 0.3	10.0 ± 2.7	58.5 ± 1.2	53.1 ± 1.3	50.5 ± 1.2	21.4 ± 1.2	26.7 ± 0.4	72.2 ± 0.6	47.0 ± 0.3	46.9 ± 1.2
SPO-Tree	21.5 ± 1.2	12.2 ± 1.6	57.4 ± 1.0	54.3 ± 0.8	50.2 ± 1.8	20.9 ± 1.2	27.3 ± 0.8	73.8 ± 0.3	47.0 ± 2.0	47.1 ± 1.6
RRPO	26.1 ± 0.9	10.0 ± 4.7	66.2 ± 6.0	<b>68.1 ± 0.1</b>	59.0 ± 5.0	20.5 ± 5.4	28.0 ± 4.0	56.9 ± 25.7	37.9 ± 18.9	33.9 ± 12.1
SRPO	24.8 ± 1.9	<b>15.6 ± 4.2</b>	<b>67.5 ± 3.5</b>	66.6 ± 2.5	59.6 ± 2.6	<b>24.7 ± 1.4</b>	28.7 ± 0.6	<b>74.8 ± 1.0</b>	<b>55.9 ± 0.6</b>	<b>54.5 ± 2.0</b>

<sup>†</sup>Base is seed-invariant (single eval, no SD).

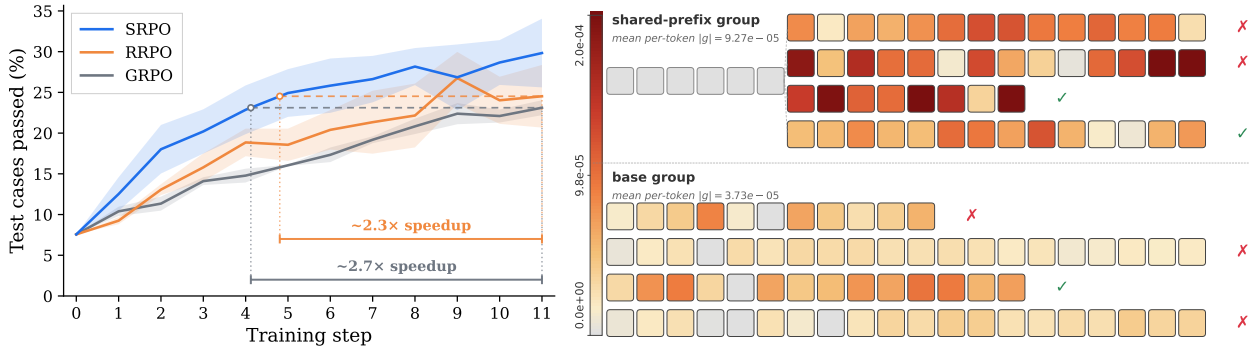


**Figure 3 Left:** SRPO converges to a higher pass rate and reaches matching pass rates 2–3× faster than GRPO and RRPO; RRPO tracks GRPO. Validation curves on LiveCodeBench v6 (medium) for OLMo-3-7B-Instruct. Shaded bands are ±1 SE. Per-method training-compute breakdown in Appendix H. **Right:** Per-thought mean of the per-token gradient signal on a single prompt under one SRPO update (1×4 split): 4 shared-prefix corrections (top) with their masked prefix and 4 base-group rollouts (bottom), illustrating where each loss assigns credit across a rollout’s tokens. Gray = masked (no gradient).

the model improves at correcting from failed prefixes its shared-prefix pass rates rise and more prompts have both groups producing signal.

*Self-localization quality.* We audit the trained SRPO checkpoint’s self-localization quality (Figure 4): for each reset-resample record we compare the model’s reset step against an oracle graded by Claude Opus 4.5, and measure the downstream correction success of the four suffix rollouts in each shared-prefix group. Figure 4 reports four observations. **(a)** On chains averaging  $\approx 17$  thought steps (capped at 20), SRPO concentrates resets in the early-middle of the reasoning chain while RRPO is approximately uniform, indicating that SRPO is actively localizing rather than resetting blindly. **(b)** Roughly half of SRPO’s localizations sit at or before Claude Opus 4.5’s failure step (clean prefix); the other half overshoot into the erroneous region. **(c)** The correction rate decays monotonically as the deviation from the oracle crosses from clean into erroneous. **(d)** Pooling across deviations, clean (Self  $\leq$  Oracle) prefixes correct nearly 2× as often as erroneous ones (28.7% vs. 16.3% Pass@4): getting the localization right is what makes the reset productive.

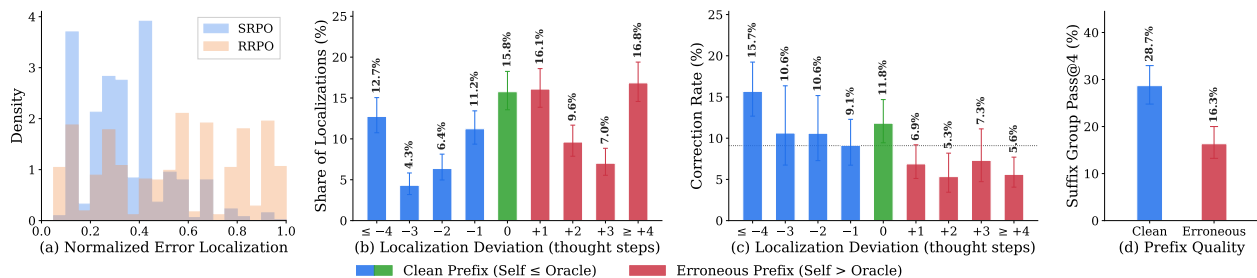


**Figure 4** Self-localization dynamics of OLMo-3-7B on coding tasks (LiveCodeBench v6 medium). (a) Self-localized vs. random reset distribution (average  $\approx 17$  thoughts per sequence). (b) Self-localization vs. frontier-model localization distribution. (c) Correction rate of self-localization by deviation from oracle (Wilson 95% CIs). (d) Pass@4 correction rate for clean vs. erroneous prefixes according to oracle.

### Takeaway

Across our experiments, self-localized resets outperform RLVR post-training with random or no resets in both final performance and sample efficiency. Self-localization itself acts as an imperfect-but-effective approximation of the credit-assignment reset oracle.

## 6 Related Work

Resets in RL have been studied primarily for exploration: Mhammedi et al. (2024) formalizes local simulator access, while DR-PO (Chang et al., 2024), Go-Explore (Ecoffet et al., 2021), and reverse curriculum generation (Florensa et al., 2018) reset to states drawn from preference data, novelty heuristics, or goal proximity. In each, the reset target is exogenous, chosen to broaden state coverage rather than to attribute credit for a failed outcome. Repurposing resets for credit assignment instead requires a step-level signal indicating *which step* of a failed trajectory to reset to. Classically this comes from value functions or process reward models (Lightman et al., 2023; Uesato et al., 2022; Wang et al., 2023; Luo et al., 2024), both requiring auxiliary trained models and either human annotation or a separate labeling pipeline. Samanta et al. (2026) show that, given thought-level reasoning, the same model can self-localize the first erroneous thought, giving a training-free step-level signal that SRPO uses to select the reset state.

The methods we compare against differ in how they use additional sampling to augment RL rollouts. Self-correction methods regenerate the full task conditioned on a prior attempt: SCoRe (Kumar et al., 2024) pairs each first attempt  $y_1$  with a second attempt  $y_2$  conditioned on it, shaping the reward by  $R(y_2) - R(y_1)$  to drive correction without changing the first-attempt distribution. Critique-GRPO (Zhang et al., 2025) augments  $G$  iid chains with a critique-conditioned refinement of each, substitutes the best refinement into the buffer, and applies an off-policy correction on refinement tokens. SRPO differs by resampling only a suffix on-policy from a verified-correct prefix, sidestepping the off-policy correction critique-conditioning requires and concentrating learning on the steps following the first error rather than re-deriving correct steps from scratch. InT (Yang et al., 2026a) also targets a localized erroneous step but replaces it with a single counterfactual, and, unlike SRPO, conditions on a human reference solution for both the localization and the counterfactual step, and uses SFT rather than RL. SPO-Tree (Guo et al., 2025) similarly intermediate states by sampling alternative continuations from cutpoints, but they use heuristics (token counts or entropy spikes) rather than self-determined semantically meaningful thought boundaries, and they use a tree based approach with cutpoints at various points of the original rollout. Beyond these methods, ASTRO (Kim et al., 2025) offers a complementary perspective on backtrack-and-resample frameworks: it uses tree search via MCTS to construct chains of thought that interleave backtracking and resampling within a single trajectory, which are then distilled into the model via SFT and refined with RL to teach it to perform such behaviors inline during generation. SRPO instead leverages backtracking and resampling as a training-time mechanism to improve credit assignment, while the resulting model continues to produce direct solutions at inference.

## 7 Limitations and Conclusion

Our methods rely on the underlying language model for initial rollouts, self-localization, correction, and thought-level reasoning, which appear sufficient at the 7B–14B scale we evaluate. Within this regime, self-localization quality is the active bottleneck: clean prefixes correct nearly  $2\times$  as often as erroneous ones (Section 5.3), and the gap to oracle-guided resets is set by localization accuracy. The methods also presume tasks that decompose into multi-step reasoning with clear reset states, and effectiveness on tasks lacking this structure is unclear. RRPO and SRPO further require verifiable rewards, and extending reset-based frameworks to non-verifiable settings (Ouyang et al., 2022; Rafailov et al., 2023; Jia et al., 2025; Zhang et al., 2026) remains an open direction. On the theory side, we establish the credit-assignment oracle’s per-iteration improvement only for a single CPI step, similarly to Kakade and Langford (2002), leaving a full convergence analysis of credit-aware policy optimization algorithms (Shani et al., 2020; Bhandari and Russo, 2021; Agarwal et al., 2021; Lan, 2023) as a next step.

Despite these limitations, this work establishes resets as a credit-assignment primitive for RL post-training of language models on sequential reasoning across math, science, strategic, commonsense, and coding benchmarks. We show that current language models already possess sufficient self-localization capability to drive meaningful improvements when used as a credit-assignment oracle. Two natural future directions follow. First, iterating on the reset mechanism itself, e.g. by training a dedicated localizer or jointly training the policy and the localizer, to close the gap to oracle-guided resets. Second, extending SRPO to long-horizon tasks with several intermediate decision points, agentic tasks, and multi-turn dialogue. In these settings, focusing learning on key decision points via reset-based credit assignment becomes increasingly important.

## References

- Alekh Agarwal, Sham M. Kakade, Jason D. Lee, and Gaurav Mahajan. On the theory of policy gradient methods: Optimality, approximation, and distribution shift. *Journal of Machine Learning Research*, 22(98):1–76, 2021.
- Jalaj Bhandari and Daniel Russo. On the linear convergence of policy gradient methods for finite MDPs. In *International Conference on Artificial Intelligence and Statistics*, pages 2386–2394. PMLR, 2021.
- Jonathan D. Chang, Wenhao Zhan, Owen Oertell, Kianté Brantley, Dipendra Misra, Jason D. Lee, and Wen Sun. Dataset Reset Policy Optimization for RLHF, April 2024. <http://arxiv.org/abs/2404.08495>. arXiv:2404.08495.
- Amir Dembo and Ofer Zeitouni. *Large Deviations Techniques and Applications*. Springer, 2nd edition, 2010.
- Adrien Ecoffet, Joost Huizinga, Joel Lehman, Kenneth O. Stanley, and Jeff Clune. First return, then explore, September 2021. <http://arxiv.org/abs/2004.12919>. arXiv:2004.12919.
- Kehua Feng, Xinyi Shen, Keyan Ding, et al. Sciknoweval: Evaluating multi-level scientific knowledge of large language models. *arXiv preprint arXiv:2406.09098*, 2024. <https://arxiv.org/abs/2406.09098>.
- Carlos Florensa, David Held, Markus Wulfmeier, Michael Zhang, and Pieter Abbeel. Reverse Curriculum Generation for Reinforcement Learning, July 2018. <http://arxiv.org/abs/1707.05300>. arXiv:1707.05300.
- Marguerite Frank and Philip Wolfe. An algorithm for quadratic programming. *Naval Research Logistics Quarterly*, 3(1–2):95–110, 1956.
- Sara A Geer. *Empirical Processes in M-estimation*, volume 6. Cambridge University Press, 2000.
- Tobias Gerstenberg. Counterfactual simulation in causal cognition. *Trends in Cognitive Sciences*, 2024. doi: 10.1016/j.tics.2024.04.012.
- Mor Geva, Daniel Khashabi, Elad Segal, Tushar Khot, Dan Roth, and Jonathan Berant. Did aristotle use a laptop? a question answering benchmark with implicit reasoning strategies. *Transactions of the Association for Computational Linguistics*, 9:246–261, 2021. <https://aclanthology.org/2021.tacl-1.21/>.
- Yiran Guo, Lijie Xu, Jie Liu, Dan Ye, and Shuang Qiu. Segment Policy Optimization: Effective Segment-Level Credit Assignment in RL for Large Language Models, May 2025. <https://arxiv.org/abs/2505.23564v2>.
- Dan Hendrycks, Collin Burns, Saurav Kadavath, Akul Arora, Steven Basart, Eric Tang, Dawn Song, and Jacob Steinhardt. Measuring mathematical problem solving with the MATH dataset. In *NeurIPS*, 2021.

- Edward J Hu, Yelong Shen, Phillip Wallis, Zeyuan Allen-Zhu, Yuanzhi Li, Shean Wang, Lu Wang, and Weizhu Chen. Lora: Low-rank adaptation of large language models. *arXiv preprint arXiv:2106.09685*, 2021.
- Naman Jain, King Han, Alex Gu, Wen-Ding Li, Fanjia Yan, Tianjun Zhang, Sida Wang, Armando Solar-Lezama, Koushik Sen, and Ion Stoica. Livecodebench: Holistic and contamination free evaluation of large language models for code. *arXiv preprint arXiv:2403.07974*, 2024.
- Ruipeng Jia, Yunyi Yang, Yongbo Gai, Kai Luo, Shihao Huang, Jianhe Lin, Xiaoxi Jiang, and Guanjun Jiang. Writing-zero: Bridge the gap between non-verifiable tasks and verifiable rewards, 2025.
- Sham Kakade and John Langford. Approximately optimal approximate reinforcement learning. In *International Conference on Machine Learning (ICML)*, pages 267–274, 2002.
- Joongwon Kim, Anirudh Goyal, Liang Tan, Hannaneh Hajishirzi, Srinivasan Iyer, and Tianlu Wang. ASTRO: Teaching Language Models to Reason by Reflecting and Backtracking In-Context, July 2025. <http://arxiv.org/abs/2507.00417>. arXiv:2507.00417.
- Aviral Kumar, Vincent Zhuang, Rishabh Agarwal, Yi Su, John D. Co-Reyes, Avi Singh, Kate Baumli, Shariq Iqbal, Colton Bishop, Rebecca Roelofs, Lei M. Zhang, Kay McKinney, Disha Shrivastava, Cosmin Paduraru, George Tucker, Doina Precup, Feryal Behbahani, and Aleksandra Faust. Training Language Models to Self-Correct via Reinforcement Learning, October 2024. <http://arxiv.org/abs/2409.12917>. arXiv:2409.12917.
- Guanghui Lan. Policy mirror descent for reinforcement learning: Linear convergence, new sampling complexity, and generalized problem classes. *Mathematical Programming*, 198(1):1059–1106, 2023.
- Jia LI, Edward Beeching, Lewis Tunstall, Ben Lipkin, Roman Soletskyi, Shengyi Costa Huang, Kashif Rasul, Longhui Yu, Albert Jiang, Ziju Shen, Zihan Qin, Bin Dong, Li Zhou, Yann Fleureau, Guillaume Lample, and Stanislas Polu. NuminaMath. [<https://huggingface.co/AI-MO/NuminaMath-CoT>]([https://github.com/project-numina/aimo-progress-prize/blob/main/report/numina\\_dataset.pdf](https://github.com/project-numina/aimo-progress-prize/blob/main/report/numina_dataset.pdf)), 2024.
- Hunter Lightman, Vineet Kosaraju, Yura Burda, Harri Edwards, Bowen Baker, Teddy Lee, Jan Leike, John Schulman, Ilya Sutskever, and Karl Cobbe. Let’s Verify Step by Step, May 2023. <https://arxiv.org/abs/2305.20050v1>.
- Zihan Liu, Zhuolin Yang, Yang Chen, Chankyu Lee, Mohammad Shoeybi, Bryan Catanzaro, and Wei Ping. Acereason-nemotron 1.1: Advancing math and code reasoning through sft and rl synergy. *arXiv preprint arXiv:2506.13284*, 2025.
- Liangchen Luo, Yinxiao Liu, Rosanne Liu, Samrat Phatale, Meiqi Guo, Harsh Lara, Yunxuan Li, Lei Shu, Yun Zhu, Lei Meng, Jiao Sun, and Abhinav Rastogi. Improve Mathematical Reasoning in Language Models by Automated Process Supervision, June 2024. <https://arxiv.org/abs/2406.06592v2>.
- Zakaria Mhammedi, Dylan J. Foster, and Alexander Rakhlin. The Power of Resets in Online Reinforcement Learning, April 2024. <http://arxiv.org/abs/2404.15417>. arXiv:2404.15417.
- Team Olmo, Allyson Ettinger, Amanda Bertsch, Bailey Kuehl, David Graham, David Heineman, Dirk Groeneveld, Faeze Brahman, Finbarr Timbers, Hamish Ivison, Jacob Morrison, Jake Poznanski, Kyle Lo, Luca Soldaini, Matt Jordan, Mayee Chen, Michael Noukhovitch, Nathan Lambert, Pete Walsh, Pradeep Dasigi, Robert Berry, Saumya Malik, Saurabh Shah, Scott Geng, Shane Arora, Shashank Gupta, Taira Anderson, Teng Xiao, Tyler Murray, Tyler Romero, Victoria Graf, Akari Asai, Akshita Bhagia, Alexander Wettig, Alisa Liu, Aman Rangapur, Chloe Anastasiades, Costa Huang, Dustin Schwenk, Harsh Trivedi, Ian Magnusson, Jaron Lochner, Jiacheng Liu, Lester James V. Miranda, Maarten Sap, Malia Morgan, Michael Schmitz, Michal Guerquin, Michael Wilson, Regan Huff, Ronan Le Bras, Rui Xin, Rulin Shao, Sam Skjonsberg, Shannon Zejiang Shen, Shuyue Stella Li, Tucker Wilde, Valentina Pyatkin, Will Merrill, Yapei Chang, Yuling Gu, Zhiyuan Zeng, Ashish Sabharwal, Luke Zettlemoyer, Pang Wei Koh, Ali Farhadi, Noah A. Smith, and Hannaneh Hajishirzi. Olmo 3, 2025. <https://arxiv.org/abs/2512.13961>.
- Long Ouyang, Jeffrey Wu, Xu Jiang, Diogo Almeida, Carroll L. Wainwright, Pamela Mishkin, Chong Zhang, Sandhini Agarwal, Katarina Slama, Alex Ray, John Schulman, Jacob Hilton, Fraser Kelton, Luke Miller, Maddie Simens, Amanda Askell, Peter Welinder, Paul Christiano, Jan Leike, and Ryan Lowe. Training language models to follow instructions with human feedback. *Advances in Neural Information Processing Systems*, 35:27730–27744, 2022.
- Rafael Rafailov, Archit Sharma, Eric Mitchell, Stefano Ermon, Christopher D. Manning, and Chelsea Finn. Direct preference optimization: Your language model is secretly a reward model. In *Advances in Neural Information Processing Systems*, volume 36, pages 53728–53741, 2023.
- Ankur Samanta, Akshayaa Magesh, Ayush Jain, Kavosh Asadi, Youliang Yu, Daniel Jiang, Boris Vidolov, Kaveh

- Hassani, Paul Sajda, Jalaj Bhandari, et al. Structure enables effective self-localization of errors in LLMs. *arXiv preprint arXiv:2602.02416*, 2026.
- John Schulman, Sergey Levine, Pieter Abbeel, Michael I. Jordan, and Philipp Moritz. Trust region policy optimization. In *International Conference on Machine Learning (ICML)*, 2015.
- John Schulman, Filip Wolski, Prafulla Dhariwal, Alec Radford, and Oleg Klimov. Proximal policy optimization algorithms. *arXiv preprint arXiv:1707.06347*, 2017.
- Lior Shani, Yonathan Efroni, and Shie Mannor. Adaptive trust region policy optimization: Global convergence and faster rates for regularized MDPs. In *Proceedings of the AAAI Conference on Artificial Intelligence*, volume 34, pages 5668–5675, 2020.
- Zhihong Shao, Peiyi Wang, Qihao Zhu, Runxin Xu, Junxiao Song, Xiao Bi, Haowei Zhang, Mingchuan Zhang, Y. K. Li, Yu Wu, and Daya Guo. DeepSeekMath: Pushing the limits of mathematical reasoning in open language models. *arXiv preprint arXiv:2402.03300*, 2024.
- Uri Sherman, Tomer Koren, and Yishay Mansour. Convergence and sample complexity of first-order methods for agnostic reinforcement learning. *arXiv preprint arXiv:2507.04406*, 2025.
- Irina G. Shevtsova. An improvement of convergence rate estimates in the Lyapunov theorem. *Doklady Mathematics*, 82(3):862–864, 2010.
- Alon Talmor, Jonathan Herzig, Nicholas Lourie, and Jonathan Berant. CommonsenseQA: A question answering challenge targeting commonsense knowledge. In *Proceedings of the 2019 Conference of the North American Chapter of the Association for Computational Linguistics*, pages 4149–4158. Association for Computational Linguistics, 2019. <https://aclanthology.org/N19-1421>.
- Manan Tomar, Lior Shani, Yonathan Efroni, and Mohammad Ghavamzadeh. Mirror descent policy optimization. *arXiv preprint arXiv:2005.09814*, 2020.
- Harvard-MIT Mathematics Tournament. Hmmt november 2025 problems and solutions, 2025. <https://www.hmmt.org/www/archive/284>. Accessed: 2026-05-06.
- Jonathan Uesato, Nate Kushman, Ramana Kumar, Francis Song, Noah Siegel, Lisa Wang, Antonia Creswell, Geoffrey Irving, and Irina Higgins. Solving math word problems with process- and outcome-based feedback, November 2022. <https://arxiv.org/abs/2211.14275v1>.
- Nino Vieillard, Olivier Pietquin, and Matthieu Geist. Deep conservative policy iteration. In *Proceedings of the AAAI Conference on Artificial Intelligence*, volume 34, pages 6070–6077, 2020.
- Kaiwen Wang, Jin Zhou, Jonathan Chang, Zhaolin Gao, Nathan Kallus, Kianté Brantley, and Wen Sun. Value-guided search for efficient chain-of-thought reasoning. *Advances in Neural Information Processing Systems*, 38:84806–84841, 2026.
- Peiyi Wang, Lei Li, Zhihong Shao, R. X. Xu, Damai Dai, Yifei Li, Deli Chen, Y. Wu, and Zhifang Sui. Math-Shepherd: Verify and Reinforce LLMs Step-by-step without Human Annotations, December 2023. <https://arxiv.org/abs/2312.08935v3>.
- Phillip P. Witkowski, Lindsay J.H. Rondot, Zeb Kurth-Nelson, Mona M. Garvert, Raymond J. Dolan, Timothy E.J. Behrens, and Erie Boorman. Neural mechanisms of credit assignment for delayed outcomes during contingent learning. *eLife*, 13:RP101841, 2025. doi: 10.7554/eLife.101841.3.
- Matthew Y. R. Yang, Hao Bai, Ian Wu, Gene Yang, Amrith Setlur, and Aviral Kumar. InT: Self-Proposed Interventions Enable Credit Assignment in LLM Reasoning, January 2026a. <https://arxiv.org/abs/2601.14209v1>.
- Matthew YR Yang, Hao Bai, Ian Wu, Gene Yang, Amrith Setlur, and Aviral Kumar. Int: Self-proposed interventions enable credit assignment in llm reasoning. *arXiv preprint arXiv:2601.14209*, 2026b.
- Qwen An Yang, Baosong Yang, Beichen Zhang, Binyuan Hui, Bo Zheng, Bowen Yu, Chengyuan Li, Dayiheng Liu, Fei Huang, Guanting Dong, Haoran Wei, Huan Lin, Jian Yang, Jianhong Tu, Jianwei Zhang, Jianxin Yang, Jiaxin Yang, Jingren Zhou, Junyang Lin, Kai Dang, Keming Lu, Keqin Bao, Kexin Yang, Le Yu, Mei Li, Mingfeng Xue, Pei Zhang, Qin Zhu, Rui Men, Runji Lin, Tianhao Li, Tingyu Xia, Xingzhang Ren, Xuancheng Ren, Yang Fan, Yang Su, Yi-Chao Zhang, Yunyang Wan, Yuqi Liu, Zeyu Cui, Zhenru Zhang, Zihan Qiu, Shanghaoran Quan, and Zekun Wang. Qwen2.5 technical report. *ArXiv*, abs/2412.15115, 2024. <https://api.semanticscholar.org/CorpusID:274859421>.

Junkai Zhang, Zihao Wang, Lin Gui, Swarnashree Mysore Sathyendra, Jaehwan Jeong, Victor Veitch, Wei Wang, Yunzhong He, Bing Liu, and Lifeng Jin. Chasing the tail: Effective rubric-based reward modeling for large language model post-training. In *International Conference on Learning Representations*, 2026.

Xiaoying Zhang, Yipeng Zhang, Hao Sun, Kaituo Feng, Chaochao Lu, Chao Yang, and Helen Meng. Critique-GRPO: Advancing LLM Reasoning with Natural Language and Numerical Feedback, June 2025. <https://arxiv.org/abs/2506.03106v6>.

# Appendix

## Appendix Contents

### Related Work

**Section 6 Related Work.** Positioning relative to prior credit-assignment, reset-based RL, and self-correction methods, and the broader CPI / iterative-improvement lineage.

### Theory and Proofs

**Section A Proofs and Tightness for Theorem 1.** Self-contained derivation of CPI-CARO’s per-iteration improvement rate and sample complexity, with supporting lemmas (Section A.1), the proof itself (Section A.2), and a variance / signal-to-noise tightness analysis (Section A.3).

### Sampler Implementation

**Section B Implementing the Credit Sampler via Rejection Sampling.** How the abstract credit-sampler oracle in the algorithm is realized as rejection sampling on the seed’s prefix, and the relationship to the self-localizer.

### Empirical

**Section C Training Details.** LoRA setup, no clipped surrogate, and the full hyperparameter table (optimization, schedule, rollout/sampling, hardware).

**Section D Prompts.** Verbatim prompts for the thought-MDP rollout template and the L2 new self-localization method revision.

**Section E Self-Localization Quality: Raw Deviation.** Companion to the main-text localization quality figure using raw step-index deviation rather than the eff5 (5-token) filter.

**Section F Full Sampling-Strategy Ablation.**  $1 \times 4$  vs.  $2 \times 4$  vs.  $1 \times 8$  comparison across both base models under a fixed 8-rollout budget.

**Section G Per-token Gradient Concentration.** Analytical bounds on within- and cross-group concentration from suffix masking, with realized values from a held-out batch.

**Section H Training Efficiency.** Per-method compute breakdown on LiveCodeBench-medium (output tokens, wall clock, generation time) for SRPO, RRPO, and GRPO.

## A Proofs and Tightness for Theorem 1

This appendix proves Theorem 1 and establishes the sharpness of its rates. The development is organized into three subsections.

*Appendix A.1: Supporting lemmas.* We state and prove the four lemmas the main proof relies on: the advantage decomposition over  $\mathcal{G}_{h,\tau}/\mathcal{G}_{h,\tau}^c$ , the credit-aware simulation lemma, the resulting credit-aware CPI bound, and a greedy-policy transfer lemma.

*Appendix A.2: Proof of Theorem 1.* We assemble these lemmas into a four-step argument: regression error,  $L^2$ -to-advantage transfer, concentration of the advantage estimator, and a case-specific CPI inequality. The random-sampler and credit-sampler cases share all four steps and differ only in the sampling distribution and which CPI bound is invoked.

*Appendix A.3: Variance, signal-to-noise, and tightness.* We bound the per-sample variance of the advantage estimator, give a signal-to-noise reading that locates the  $p_\pi^2$  factor in the sample-complexity gap, and exhibit a finite-horizon MDP on which both rates in Theorem 1 are tight up to absolute constants.

Throughout, we work in the finite-horizon MDP  $(\mathcal{X}, \mathcal{Y}, P, r, H, \mu)$  of Section 2 and adopt the notation of Section 3:  $\mathcal{G}_{h,\tau}$  is the  $\tau$ -improvable set at time  $h$ ,  $p_{\pi,h} = \mathbb{P}_{x \sim d_\pi^h}[x \in \mathcal{G}_{h,\tau}]$ ,  $p_\pi = \frac{1}{H} \sum_{h=1}^H p_{\pi,h}$ , and  $\pi_{\mathcal{G}}$  is the credit-assignment greedy policy that plays  $\pi^+$  on  $\mathcal{G}_{h,\tau}$  and  $\pi$  elsewhere. For any policy  $\pi'$ , recall the conditional policy advantages

$$\mathbb{A}_{\pi,\mu}^{\mathcal{G}}(\pi') := \mathbb{E}[A_h^\pi(x, y) \mid x \in \mathcal{G}_{h,\tau}], \quad \mathbb{A}_{\pi,\mu}^{\mathcal{G}^c}(\pi') := \mathbb{E}[A_h^\pi(x, y) \mid x \notin \mathcal{G}_{h,\tau}],$$

with both expectations taken under  $h \sim \text{Unif}[H]$ ,  $x \sim d_\pi^h$ ,  $y \sim \pi'_h(\cdot \mid x)$ .

### A.1 Supporting Lemmas

*Advantage decomposition.*

**Lemma 2** (Advantage decomposition). *For any policy  $\pi'$ ,*

$$\mathbb{A}_{\pi,\mu}(\pi') = p_\pi \mathbb{A}_{\pi,\mu}^{\mathcal{G}}(\pi') + (1 - p_\pi) \mathbb{A}_{\pi,\mu}^{\mathcal{G}^c}(\pi'). \quad (3)$$

*For the credit-assignment greedy policy  $\pi_{\mathcal{G}}$ , the  $\mathcal{G}_{h,\tau}^c$  term vanishes and*

$$\mathbb{A}_{\pi,\mu}(\pi_{\mathcal{G}}) = p_\pi \mathbb{A}_{\pi,\mu}^{\mathcal{G}}(\pi^+) \geq \tau p_\pi. \quad (4)$$

*Proof.* Equation (3) is the law of total expectation applied to the partition  $\{\mathcal{G}_{h,\tau}, \mathcal{G}_{h,\tau}^c\}$  under the joint distribution  $(h, x, y) \sim \text{Unif}[H] \times d_\pi^h \times \pi'_h$ . For equation (4): on  $\mathcal{G}_{h,\tau}$ ,  $(\pi_{\mathcal{G}})_h(\cdot \mid x) = \pi_h(\cdot \mid x)$ , so  $\mathbb{E}_{y \sim (\pi_{\mathcal{G}})_h}[A_h^\pi(x, y)] = \mathbb{E}_{y \sim \pi_h}[A_h^\pi(x, y)] = 0$ . On  $\mathcal{G}_{h,\tau}^c$ ,  $(\pi_{\mathcal{G}})_h = \pi_h^+$  and  $\mathbb{E}_{y \sim \pi_h^+}[A_h^\pi(x, y)] = \max_y A_h^\pi(x, y) \geq \tau$  by definition of  $\mathcal{G}_{h,\tau}$ .  $\square$

*Credit-aware simulation lemma.* The classical CPI bound (Kakade and Langford, 2002) controls state-distribution drift between  $\pi$  and a mixture  $\pi_\alpha = (1 - \alpha)\pi + \alpha\pi'$  by a quantity  $\propto \alpha H^2$ , derived from the worst-case TV deviation  $\|\pi'_h - \pi_h\|_{\text{TV}}(x) \leq 1$ . When  $\pi'$  agrees with  $\pi$  off  $\mathcal{G}_{h,\tau}$ , the same argument yields a tighter bound that carries an extra  $p_\pi$  factor.

**Lemma 3** (Credit-aware state-distribution simulation). *Let  $\pi'$  be any policy with  $\pi'_h(\cdot \mid x) = \pi_h(\cdot \mid x)$  for all  $h \in [H]$  and  $x \notin \mathcal{G}_{h,\tau}$ , and let  $\pi_\alpha = (1 - \alpha)\pi + \alpha\pi'$  for  $\alpha \in [0, 1]$ . Then*

$$\sum_{h=1}^H \|d_{\pi_\alpha}^h - d_\pi^h\|_{\text{TV}} \leq \alpha H^2 p_\pi. \quad (5)$$

*Proof.* We invoke the standard simulation lemma in the form

$$J_r(\pi_\alpha) - J_r(\pi) = \alpha \sum_{h''=1}^H \mathbb{E}_{x \sim d_{\pi}^{h''}} \left[ \left( \pi'_{h''}(\cdot | x) - \pi_{h''}(\cdot | x) \right)^\top Q_{h''}^{\pi_\alpha, r}(x, \cdot) \right], \quad (6)$$

which follows from the performance-difference identity (Kakade and Langford, 2002) by recursively expanding  $V_1^{\pi_\alpha} - V_1^\pi$  along trajectories drawn under  $\pi$ .

For any state  $s$  and time  $h \in [H]$ , the visitation  $d_\pi^h(s) = \mathbb{E}_\pi[\mathbf{1}\{x_h = s\}]$  is the expected return of  $\pi$  under the indicator reward  $\mathbf{1}\{x_h = s\}$  that fires once when the trajectory visits state  $s$  at time  $h$ . The corresponding Q-function is

$$Q_{h''}^{\pi_\alpha, \mathbf{1}\{x_h=s\}}(x, y) = \Pr_{\pi_\alpha}(x_h = s | x_{h''} = x, y_{h''} = y) \in [0, 1]$$

for  $h'' \leq h$  (and zero for  $h'' > h$ ). Summing over  $s$ , the trajectory passes through some state at time  $h$  with probability one, so

$$\sum_{s \in \mathcal{X}} Q_{h''}^{\pi_\alpha, \mathbf{1}\{x_h=s\}}(x, y) = 1 \quad \text{for all } (x, y, h'') \text{ with } h'' \leq h. \quad (7)$$

Apply equation (6) with  $r = \mathbf{1}\{x_h = s\}$ . Writing  $\Delta_{h''}(\cdot | x) := \pi'_{h''}(\cdot | x) - \pi_{h''}(\cdot | x)$ , taking absolute values, summing over  $s$ , and using  $Q^{(s)} \geq 0$  together with equation (7),

$$\begin{aligned} \sum_s |d_{\pi_\alpha}^h(s) - d_\pi^h(s)| &\leq \alpha \sum_{h''=1}^h \mathbb{E}_{x \sim d_{\pi}^{h''}} \left[ \sum_s \left| \sum_y \Delta_{h''}(y | x) Q_{h''}^{\pi_\alpha, \mathbf{1}\{x_h=s\}}(x, y) \right| \right] \\ &\leq \alpha \sum_{h''=1}^h \mathbb{E}_{x \sim d_{\pi}^{h''}} \left[ \sum_y |\Delta_{h''}(y | x)| \underbrace{\sum_s Q_{h''}^{\pi_\alpha, \mathbf{1}\{x_h=s\}}(x, y)}_{=1} \right] \\ &= \alpha \sum_{h''=1}^h \mathbb{E}_{x \sim d_{\pi}^{h''}} [\|\Delta_{h''}(\cdot | x)\|_1]. \end{aligned}$$

By assumption of the lemma,  $\pi'_{h''}(\cdot | x) = \pi_{h''}(\cdot | x)$  for  $x \notin \mathcal{G}_{h, \tau}$ , hence  $\|\Delta_{h''}(\cdot | x)\|_1 \leq 2 \mathbf{1}\{x \in \mathcal{G}_{h, \tau}\}$ , giving

$$\sum_s |d_{\pi_\alpha}^h(s) - d_\pi^h(s)| \leq 2\alpha \sum_{h''=1}^h p_{\pi, h''}.$$

Since  $\|d_{\pi_\alpha}^h - d_\pi^h\|_{\text{TV}} = \frac{1}{2} \sum_s |d_{\pi_\alpha}^h(s) - d_\pi^h(s)|$ , we obtain  $\|d_{\pi_\alpha}^h - d_\pi^h\|_{\text{TV}} \leq \alpha \sum_{h''=1}^h p_{\pi, h''}$ . Summing over  $h$ ,

$$\sum_{h=1}^H \|d_{\pi_\alpha}^h - d_\pi^h\|_{\text{TV}} \leq \alpha \sum_{h=1}^H \sum_{h''=1}^h p_{\pi, h''} \leq \alpha H \sum_{h''=1}^H p_{\pi, h''} = \alpha H^2 p_\pi. \quad \square$$

*Classical CPI improvement bound.* For completeness and as a baseline for the credit-aware refinement below, we state the classical CPI improvement bound (Kakade and Langford, 2002) in its finite-horizon form. We use this lemma in the random-sampler case of the proof of Theorem 1.

**Lemma 4** (Classical CPI improvement bound; Kakade and Langford, 2002). *For any policy  $\pi'$  and any  $\alpha \in [0, 1]$ , let  $\pi_\alpha = (1 - \alpha)\pi + \alpha\pi'$  and  $\epsilon_{\text{CPI}} := \max_{h, x} |\mathbb{E}_{y \sim \pi'_h(\cdot | x)} [A_h^\pi(x, y)]|$ . Then*

$$J(\pi_\alpha) - J(\pi) \geq \alpha H \mathbb{A}_{\pi, \mu}(\pi') - \frac{\alpha^2 H^2 \epsilon_{\text{CPI}}}{2}, \quad \epsilon_{\text{CPI}} \leq H R_{\max}. \quad (8)$$

*Credit-aware CPI bound.* Plugging Lemma 3 into the performance-difference identity yields a CPI-style improvement bound whose quadratic error term carries an extra  $p_\pi$  factor.

**Corollary 5** (Credit-aware CPI bound). *Under the conditions of Lemma 3, with  $\epsilon_{\text{CPI}}^\tau := \max_{h,x} |\mathbb{E}_{y \sim \pi'_h(\cdot|x)}[A_h^\pi(x,y)]|$ ,*

$$J(\pi_\alpha) - J(\pi) \geq \alpha H p_\pi \mathbb{A}_{\pi,\mu}^{\mathcal{G}}(\pi') - \alpha^2 H^2 p_\pi \epsilon_{\text{CPI}}^\tau. \quad (9)$$

*Proof.* By the performance-difference lemma applied to  $\pi_\alpha$  versus  $\pi$ , and using  $\mathbb{E}_{y \sim \pi_h(\cdot|x)}[A_h^\pi(x,y)] = 0$  together with the linearity of  $\pi_\alpha$  in  $\pi'$ ,

$$J(\pi_\alpha) - J(\pi) = \alpha \sum_{h=1}^H \mathbb{E}_{x \sim d_{\pi_\alpha}^h} [\bar{A}_h^\pi(x)], \quad \bar{A}_h^\pi(x) := \mathbb{E}_{y \sim \pi'_h(\cdot|x)} [A_h^\pi(x,y)].$$

Splitting the expectation under  $d_{\pi_\alpha}^h$  into its  $d_\pi^h$  component plus an error,

$$\begin{aligned} J(\pi_\alpha) - J(\pi) &= \alpha \sum_{h=1}^H \mathbb{E}_{d_\pi^h} [\bar{A}_h^\pi] + \alpha \sum_{h=1}^H (\mathbb{E}_{d_{\pi_\alpha}^h} [\bar{A}_h^\pi] - \mathbb{E}_{d_\pi^h} [\bar{A}_h^\pi]) \\ &\geq \alpha H \mathbb{A}_{\pi,\mu}(\pi') - \alpha \epsilon_{\text{CPI}}^\tau \sum_{h=1}^H \|d_{\pi_\alpha}^h - d_\pi^h\|_{\text{TV}}, \end{aligned}$$

where the first term uses the definition of  $\mathbb{A}_{\pi,\mu}(\pi')$  and the second applies  $|\mathbb{E}_p f - \mathbb{E}_q f| \leq \|f\|_\infty \|p - q\|_{\text{TV}}$  for non-negative  $f$  (here  $\bar{A}_h^\pi \geq 0$  since  $\pi'_h$  agrees with the greedy policy on  $\mathcal{G}_{h,\tau}$  and with  $\pi_h$  elsewhere, so  $\bar{A}_h^\pi(x) = \max_y A_h^\pi(x,y) \geq 0$  on  $\mathcal{G}_{h,\tau}$  and  $\bar{A}_h^\pi(x) = 0$  on  $\mathcal{G}_{h,\tau}^c$ ). By Lemma 2,  $\mathbb{A}_{\pi,\mu}(\pi') = p_\pi \mathbb{A}_{\pi,\mu}^{\mathcal{G}}(\pi')$  since  $\pi'$  agrees with  $\pi$  off  $\mathcal{G}_{h,\tau}$ . Substituting Lemma 3 into the error term yields equation (9).  $\square$

*Greedy-policy transfer.* The algorithm uses the empirical greedy policy  $\hat{\pi}_h^+(x) := \arg \max_y \hat{Q}(x,y,h)$  in place of the true greedy  $\pi_h^+$ . The next lemma controls the loss from this substitution.

**Lemma 6** (Greedy-policy transfer). *Let  $\hat{Q} : \mathcal{X} \times \mathcal{Y} \times [H] \rightarrow \mathbb{R}$  be any function and define  $\hat{\pi}_h^+(x) := \arg \max_{y \in \mathcal{Y}} \hat{Q}(x,y,h)$ . For every  $h \in [H]$  and  $x \in \mathcal{X}$ ,*

$$A_h^\pi(x, \hat{\pi}_h^+(x)) \geq A_h^\pi(x, \pi_h^+(x)) - 2 \sup_{y \in \mathcal{Y}} |\hat{Q}(x,y,h) - Q_h^\pi(x,y)|. \quad (10)$$

*Proof.* Let  $\Delta(y) := |\hat{Q}(x,y,h) - Q_h^\pi(x,y)|$  and write  $y^+ = \pi_h^+(x)$ ,  $\hat{y}^+ = \hat{\pi}_h^+(x)$ . By the empirical greedy property,  $\hat{Q}(x, \hat{y}^+, h) \geq \hat{Q}(x, y^+, h)$ , so

$$\begin{aligned} Q_h^\pi(x, \hat{y}^+) &\geq \hat{Q}(x, \hat{y}^+, h) - \Delta(\hat{y}^+) \\ &\geq \hat{Q}(x, y^+, h) - \Delta(\hat{y}^+) \\ &\geq Q_h^\pi(x, y^+) - \Delta(y^+) - \Delta(\hat{y}^+) \\ &\geq Q_h^\pi(x, y^+) - 2 \sup_y \Delta(y). \end{aligned}$$

Subtracting  $V_h^\pi(x)$  from both sides yields equation (10).  $\square$

*Least-squares regression error.* The proof of Theorem 1 fits  $\hat{Q}$  by least-squares regression on the Q-rollout targets. Under realizability and a finite hypothesis class, the resulting error obeys a fast rate that is standard in the empirical-risk-minimization literature (Geer, 2000).

**Lemma 7** (Least-squares regression error for finite, realizable classes). *Let  $\mathcal{F}$  be a finite class of functions  $\mathcal{X} \times \mathcal{Y} \times [H] \rightarrow [0, HR_{\max}]$  and suppose  $Q_h^\pi \in \mathcal{F}$  for every  $h \in [H]$  (realizability). Let  $d$  be any distribution over  $(x,y,h)$ , let  $\{(x_i, y_i, h_i)\}_{i=1}^n \stackrel{\text{i.i.d.}}{\sim} d$ , and let  $\hat{Q}_i$  be conditionally unbiased estimates of  $Q_{h_i}^\pi(x_i, y_i)$  with*

$\hat{Q}_i \in [0, HR_{\max}]$  a.s. Define  $\hat{Q} := \arg \min_{f \in \mathcal{F}} \sum_{i=1}^n (f(x_i, y_i, h_i) - \hat{Q}_i)^2$ . For any  $\delta \in (0, 1)$ , with probability at least  $1 - \delta$ ,

$$\mathbb{E}_{(x,y,h) \sim d} \left[ (\hat{Q}(x, y, h) - Q_h^\pi(x, y))^2 \right] \leq \frac{C_0 H^2 R_{\max}^2 \log(|\mathcal{F}|/\delta)}{n}, \quad (11)$$

for an absolute constant  $C_0$ .

*Sketch.* This is the standard fast-rate bound for ERM over a finite, realizable function class with bounded targets, obtained by combining a Bernstein-type concentration inequality applied to  $(f(x, y, h) - \hat{Q})^2 - (Q_h^\pi(x, y) - \hat{Q})^2$  for each fixed  $f \in \mathcal{F}$  with a union bound over  $\mathcal{F}$ ; see, e.g., Geer (2000). The realizability hypothesis  $Q_h^\pi \in \mathcal{F}$  removes the approximation error and yields the  $1/n$  (rather than  $1/\sqrt{n}$ ) fast rate.  $\square$

## A.2 Proof of Theorem 1

We prove the two cases of Theorem 1 via a common pipeline: (i) least-squares regression error, (ii) transfer from  $L^2$ -error on  $\hat{Q}$  to advantage error of  $\hat{\pi}^+$ , and (iii) plugging the resulting advantage lower bound into the appropriate CPI inequality. The cases differ only in the sampling distribution and which CPI inequality is applied.

*Setup.* Let  $d$  denote the sampling distribution over  $(x, y, h)$ :  $d = d_\pi^h \times \text{Unif}(\mathcal{Y}) \times \text{Unif}[H]$  for the random sampler (CPI-RR), and  $d = (d_\pi^h \mid x \in \mathcal{G}_{h,\tau}) \times \text{Unif}(\mathcal{Y}) \times \text{Unif}[H]$  for the credit sampler (CPI-CARO). The Q-rollout  $\text{QROLLOUT}(\pi, x_i, y_i, h_i)$  returns  $\hat{Q}_i$  with  $\mathbb{E}[\hat{Q}_i \mid x_i, y_i, h_i] = Q_{h_i}^\pi(x_i, y_i)$  and  $\hat{Q}_i \in [0, HR_{\max}]$  (per-step rewards lie in  $[0, R_{\max}]$  and are non-negative). For any policy  $\pi'$ , define the *policy advantage under  $d$*  as

$$\mathbb{A}_d(\pi') := \mathbb{E}_{(x,h) \sim d_{x,h}} \mathbb{E}_{y \sim \pi'_h(\cdot|x)} [A_h^\pi(x, y)],$$

where  $d_{x,h}$  denotes the marginal of  $d$  on  $(x, h)$ . In particular,

$$\begin{aligned} \mathbb{A}_d(\pi') &= \mathbb{A}_{\pi,\mu}(\pi') && \text{(random sampler),} \\ \mathbb{A}_d(\pi') &= \mathbb{A}_{\pi,\mu}^{\mathcal{G}}(\pi') && \text{(credit sampler).} \end{aligned}$$

This unified notation lets Steps 1–3 below be stated once for both samplers, with the two cases distinguished only in Step 4 via the identities above.

The algorithm uses the empirical greedy policy  $\hat{\pi}_h^+(x) = \arg \max_y \hat{Q}(x, y, h)$  derived from the fitted  $\hat{Q}$  rather than the true greedy  $\pi_h^+$ . The proof tracks this substitution: Step 2 bounds the resulting advantage error via Lemma 6, Step 3 controls concentration of  $\hat{\mathbb{A}}$  around  $\mathbb{A}_d(\hat{\pi}^+)$  (not  $\mathbb{A}_d(\pi^+)$ ), and Step 4 plugs  $\hat{\pi}^+$  (or  $\hat{\pi}_{\mathcal{G}}$ ) into the appropriate CPI bound.

*Step 1: Least-squares regression error.* Lemma 7 applied with confidence parameter  $\delta/2$  gives, with probability at least  $1 - \delta/2$ ,

$$\mathbb{E}_{(x,y,h) \sim d} \left[ (\hat{Q}(x, y, h) - Q_h^\pi(x, y))^2 \right] \leq \hat{\epsilon}^2, \quad \hat{\epsilon}^2 := \frac{C_0 H^2 R_{\max}^2 \log(2|\mathcal{F}|/\delta)}{n}. \quad (12)$$

*Step 2: From  $L^2$  error to advantage error.* Lemma 6 gives, pointwise in  $(x, h)$ ,

$$A_h^\pi(x, \pi_h^+(x)) - A_h^\pi(x, \hat{\pi}_h^+(x)) \leq 2 \sup_{y \in \mathcal{Y}} |\hat{Q}(x, y, h) - Q_h^\pi(x, y)|.$$

Taking expectations under  $d$ ,

$$|\mathbb{A}_d(\hat{\pi}^+) - \mathbb{A}_d(\pi^+)| \leq 2 \mathbb{E}_{(x,h) \sim d} \left[ \sup_y |\hat{Q}(x, y, h) - Q_h^\pi(x, y)| \right] \leq 2\sqrt{|\mathcal{Y}|} \hat{\epsilon}, \quad (13)$$

where  $\mathbb{A}_d(\pi')$  denotes the policy advantage under sampling distribution  $d$ . To obtain the last step, set  $\Delta(x, y, h) := |\hat{Q}(x, y, h) - Q_h^\pi(x, y)|$  and let  $d_{x,h}$  denote the marginal of  $d$  on  $(x, h)$ . Since  $y$  is uniform on  $\mathcal{Y}$  under  $d$  conditional on  $(x, h)$ , for each fixed  $(x, h)$  the sup- $L^2$  inequality on the finite action set gives

$$\sup_{y \in \mathcal{Y}} \Delta(x, y, h) \leq \sqrt{|\mathcal{Y}| \mathbb{E}_{y \sim \text{Unif}(\mathcal{Y})} [\Delta(x, y, h)^2]}.$$

Taking expectation over  $(x, h) \sim d_{x,h}$  and applying Jensen's inequality,

$$\mathbb{E}_{(x,h) \sim d_{x,h}} \left[ \sup_y \Delta(x, y, h) \right] \leq \sqrt{|\mathcal{Y}| \mathbb{E}_{(x,y,h) \sim d} [\Delta(x, y, h)^2]} \leq \sqrt{|\mathcal{Y}|} \hat{\epsilon},$$

where the last inequality is equation (12).

*Step 3: Concentration of  $\hat{\mathbb{A}}$ .* The algorithm's plug-in advantage estimate is  $\hat{\mathbb{A}} = \frac{1}{n} \sum_{i=1}^n |\mathcal{Y}| (\hat{\pi}_{h_i}^+(y_i | x_i) - \pi_{h_i}(y_i | x_i)) \hat{Q}(x_i, y_i, h_i)$ . The empirical greedy  $\hat{\pi}^+$  is data-dependent, so a direct Hoeffding bound on  $\hat{\mathbb{A}}$  for a fixed policy does not apply. Instead, observe that  $\hat{\pi}^+ \in \Pi_{\mathcal{F}} := \{\arg \max_y f(\cdot, \cdot, \cdot) : f \in \mathcal{F}\}$ , so  $|\Pi_{\mathcal{F}}| \leq |\mathcal{F}|$ . Applying Hoeffding's inequality to each fixed  $\pi' \in \Pi_{\mathcal{F}}$  together with the variance bound of Lemma 8, and union-bounding over  $\Pi_{\mathcal{F}}$ , with probability at least  $1 - \delta/2$ ,

$$\sup_{\pi' \in \Pi_{\mathcal{F}}} |\hat{\mathbb{A}}(\pi') - \mathbb{A}_d(\pi')| \leq C_1 HR_{\max} \sqrt{\frac{|\mathcal{Y}| \log(2|\mathcal{F}|/\delta)}{n}} \leq \sqrt{|\mathcal{Y}|} \hat{\epsilon}, \quad (14)$$

where the absolute constant  $C_1 \leq \sqrt{C_0}$  has been absorbed into  $\hat{\epsilon}$  defined in equation (12). Specializing to  $\pi' = \hat{\pi}^+$  and combining with equation (13),

$$|\hat{\mathbb{A}} - \mathbb{A}_d(\pi^+)| \leq 3\sqrt{|\mathcal{Y}|} \hat{\epsilon}. \quad (15)$$

*Step 4: Apply the appropriate CPI bound.*

**Random sampler (CPI-RR).** Here  $d = d_{\pi}^h \times \text{Unif}(\mathcal{Y}) \times \text{Unif}[H]$ , so  $\mathbb{A}_d(\pi^+) = \mathbb{A}_{\pi, \mu}(\pi^+) \geq \tau p_{\pi}$  by Lemma 2 (specifically,  $\mathbb{A}_{\pi, \mu}(\pi^+) \geq \mathbb{A}_{\pi, \mu}(\pi_{\mathcal{G}}) \geq \tau p_{\pi}$ ). Choose  $n$  so that  $3\sqrt{|\mathcal{Y}|} \hat{\epsilon} \leq \tau p_{\pi}/2$ , i.e.,  $\hat{\epsilon}^2 \leq \tau^2 p_{\pi}^2 / (36|\mathcal{Y}|)$ . By equation (12), this is implied by

$$n \geq \frac{C |\mathcal{Y}| H^2 R_{\max}^2 \log(2|\mathcal{F}|/\delta)}{\tau^2 p_{\pi}^2}$$

for a universal constant  $C = 36C_0$ . On the resulting  $1 - \delta$  event, two lower bounds hold. From equation (15) and  $\mathbb{A}_d(\pi^+) = \mathbb{A}_{\pi, \mu}(\pi^+) \geq \tau p_{\pi}$ ,

$$\hat{\mathbb{A}} \geq \mathbb{A}_d(\pi^+) - 3\sqrt{|\mathcal{Y}|} \hat{\epsilon} \geq \tau p_{\pi} - \tau p_{\pi}/2 = \tau p_{\pi}/2.$$

From equation (13) and the same identity,

$$\mathbb{A}_{\pi, \mu}(\hat{\pi}^+) = \mathbb{A}_d(\hat{\pi}^+) \geq \mathbb{A}_d(\pi^+) - 2\sqrt{|\mathcal{Y}|} \hat{\epsilon} \geq \tau p_{\pi} - \tau p_{\pi}/3 \geq \tau p_{\pi}/2.$$

The algorithm returns  $\pi_{\hat{\alpha}} = (1 - \hat{\alpha})\pi + \hat{\alpha}\hat{\pi}^+$ , the convex combination of  $\pi$  with the empirical greedy  $\hat{\pi}^+$ . Applying Lemma 4 with  $\pi' = \hat{\pi}^+$  and the algorithm's choice  $\hat{\alpha} = \min\{1, \hat{\mathbb{A}}/(H^2 R_{\max})\}$  and using  $\epsilon_{\text{CPI}} \leq HR_{\max}$ ,

$$\begin{aligned} J(\pi_{\hat{\alpha}}) - J(\pi) &\geq \frac{\hat{\mathbb{A}}(2\mathbb{A}_{\pi, \mu}(\hat{\pi}^+) - \hat{\mathbb{A}})}{2HR_{\max}} \\ &\geq \frac{(\tau p_{\pi}/2)(\tau p_{\pi}/2)}{2HR_{\max}} = \frac{\tau^2 p_{\pi}^2}{8HR_{\max}}, \end{aligned}$$

where in the second line we used  $\hat{\mathbb{A}} \geq \tau p_{\pi}/2$  and  $2\mathbb{A}_{\pi, \mu}(\hat{\pi}^+) - \hat{\mathbb{A}} \geq \tau p_{\pi}/2$  (applying equation (15) a second time:  $\hat{\mathbb{A}} \leq \mathbb{A}_{\pi, \mu}(\hat{\pi}^+) + \tau p_{\pi}/2 \leq 2\mathbb{A}_{\pi, \mu}(\hat{\pi}^+) - \tau p_{\pi}/2$  when  $\mathbb{A}_{\pi, \mu}(\hat{\pi}^+) \geq \tau p_{\pi}$ ).

**Credit sampler (CPI-CARO).** Here  $d = (d_{\pi}^h | \mathcal{G}_{h, \tau}) \times \text{Unif}(\mathcal{Y}) \times \text{Unif}[H]$ , so  $\mathbb{A}_d(\pi^+) = \mathbb{A}_{\pi, \mu}^{\mathcal{G}}(\pi^+) \geq \tau$ . Choose  $n$  so that  $3\sqrt{|\mathcal{Y}|} \hat{\epsilon} \leq \tau/2$ , i.e.,

$$n \geq \frac{C |\mathcal{Y}| H^2 R_{\max}^2 \log(2|\mathcal{F}|/\delta)}{\tau^2}.$$

On the resulting  $1 - \delta$  event, two lower bounds hold. From equation (15) and  $\mathbb{A}_d(\pi^+) = \mathbb{A}_{\pi, \mu}^{\mathcal{G}}(\pi^+) \geq \tau$ ,

$$\hat{\mathbb{A}} \geq \mathbb{A}_d(\pi^+) - 3\sqrt{|\mathcal{Y}|}\hat{\epsilon} \geq \tau - \tau/2 = \tau/2.$$

From equation (13) and the same identity,

$$\mathbb{A}_{\pi, \mu}^{\mathcal{G}}(\hat{\pi}^+) = \mathbb{A}_d(\hat{\pi}^+) \geq \mathbb{A}_d(\pi^+) - 2\sqrt{|\mathcal{Y}|}\hat{\epsilon} \geq \tau - \tau/3 \geq \tau/2.$$

The algorithm returns  $\pi_{\hat{\alpha}} = (1 - \hat{\alpha})\pi + \hat{\alpha}\hat{\pi}_{\mathcal{G}}$  where  $\hat{\pi}_{\mathcal{G}}$  agrees with  $\hat{\pi}^+$  on  $\mathcal{G}_{h, \tau}$  and with  $\pi$  elsewhere, so it satisfies the hypothesis of Lemma 3. Applying Corollary 5 with  $\pi' = \hat{\pi}_{\mathcal{G}}$ ,  $\epsilon_{\text{CPI}}^{\tau} \leq HR_{\max}$ , and the algorithm's  $\hat{\alpha} = \min\{1, \hat{\mathbb{A}}/(2H^2R_{\max})\}$ ,

$$\begin{aligned} J(\pi_{\hat{\alpha}}) - J(\pi) &\geq \hat{\alpha} H p_{\pi} \mathbb{A}_{\pi, \mu}^{\mathcal{G}}(\hat{\pi}^+) - \hat{\alpha}^2 H^2 p_{\pi} \epsilon_{\text{CPI}}^{\tau} \\ &\geq \frac{p_{\pi} \hat{\mathbb{A}} (2 \mathbb{A}_{\pi, \mu}^{\mathcal{G}}(\hat{\pi}^+) - \hat{\mathbb{A}})}{4HR_{\max}} \geq \frac{p_{\pi} (\tau/2)(\tau/2)}{4HR_{\max}} = \frac{\tau^2 p_{\pi}}{16HR_{\max}}, \end{aligned}$$

where the second inequality plugs in  $\hat{\alpha}$  and uses  $\epsilon_{\text{CPI}}^{\tau} \leq HR_{\max}$ , and the third uses  $\hat{\mathbb{A}} \geq \tau/2$  and  $2\mathbb{A}_{\pi, \mu}^{\mathcal{G}}(\hat{\pi}^+) - \hat{\mathbb{A}} \geq \tau/2$  (by the same argument as in the random case, with  $\tau p_{\pi}$  replaced by  $\tau$ ).

A union bound over the  $1 - \delta/2$  events in equations (12) and (14) yields the stated  $1 - \delta$  probability in both cases.  $\square$

### A.3 Variance, Signal-to-Noise, and Tightness

The central result of this subsection is Proposition 10, which shows that the random-sampler's empirical advantage estimator requires  $\Omega(|\mathcal{Y}| R_{\max}^2 / (\tau^2 p_{\pi}^2))$  samples to certify a non-trivial lower bound, matching the upper bound for CPI-RR in Theorem 1. This shows the  $1/p_{\pi}^2$  separation between CPI-RR and CPI-CARO is a genuine algorithmic improvement — the credit-assignment oracle removes a  $p_{\pi}^2$  factor that the on-policy random-reset estimator provably cannot.

*Variance.* For both samplers, the per-sample term  $Y_i := |\mathcal{Y}|(\hat{\pi}_{h_i}^+(y_i | x_i) - \pi_{h_i}(y_i | x_i))\hat{Q}(x_i, y_i, h_i)$  of the advantage estimator  $\hat{\mathbb{A}} = \frac{1}{n} \sum_i Y_i$  is bounded by  $|\mathcal{Y}|HR_{\max}$  almost surely, and its variance is bounded uniformly by  $\sigma^2 := 2|\mathcal{Y}|H^2R_{\max}^2$ .

**Lemma 8** (Variance of  $Y_i$ ). *For both the random sampler and the credit sampler,  $\text{Var}(Y_i) \leq \mathbb{E}[Y_i^2] \leq 2|\mathcal{Y}|H^2R_{\max}^2$ .*

*Proof.* Since  $\hat{Q}_i \in [0, HR_{\max}]$ ,  $\hat{Q}$  takes values in  $[0, HR_{\max}]$  as well, so  $\mathbb{E}[Y_i^2] \leq |\mathcal{Y}|^2 H^2 R_{\max}^2 \cdot \mathbb{E}_{(x, y, h) \sim d}[(\hat{\pi}_h^+(y | x) - \pi_h(y | x))^2]$ . For each fixed  $(x, h)$ , the inner expectation under  $y \sim \text{Unif}(\mathcal{Y})$  is at most  $2/|\mathcal{Y}|$  (the sum equals  $(1 - \pi_h(\hat{\pi}_h^+(x) | x))^2 + \sum_{y \neq \hat{\pi}_h^+(x)} \pi_h(y | x)^2 \leq 2$  since  $\hat{\pi}_h^+$  is deterministic). Combining yields  $\mathbb{E}[Y_i^2] \leq 2|\mathcal{Y}|H^2R_{\max}^2$ , uniformly in the conditioning event.  $\square$

*Signal-to-noise.* The two samplers share the same noise  $\sigma^2$ , so the sample-complexity separation between CPI-RR and CPI-CARO in Theorem 1 comes from the *signal*: the magnitude of the target each estimator pursues. CPI-RR estimates  $\mathbb{A}_{\pi, \mu}(\hat{\pi}^+) \geq \tau p_{\pi}$ , so certifying  $\hat{\mathbb{A}} \geq \tau p_{\pi}/2$  requires precision  $\Theta(\tau p_{\pi})$  and hence  $n \gtrsim \sigma^2 / (\tau p_{\pi})^2 \propto |\mathcal{Y}|H^2R_{\max}^2 / (\tau^2 p_{\pi}^2)$  samples. CPI-CARO estimates the conditional advantage  $\mathbb{A}_{\pi, \mu}^{\mathcal{G}}(\hat{\pi}^+) \geq \tau$  directly on  $\mathcal{G}_{h, \tau}$ , so precision  $\Theta(\tau)$  suffices and  $n \gtrsim \sigma^2 / \tau^2 \propto |\mathcal{Y}|H^2R_{\max}^2 / \tau^2$ , *independent of  $p_{\pi}$* . Same noise,  $1/p_{\pi}$ -larger signal: the  $p_{\pi}^2$  factor in CPI-RR's sample complexity is the squared signal-to-noise ratio of the two targets, not a variance gap. The next subsection makes this  $1/p_{\pi}^2$  tightness precise via an explicit single-step ( $H = 1$ ) construction.

*Formalizing the signal-to-noise gap.* We exhibit a single-step ( $H = 1$ ) MDP on which the random-sampler's empirical-mean advantage estimator  $\hat{\mathbb{A}}$  requires  $\Omega(|\mathcal{Y}| R_{\max}^2 / (\tau^2 p_{\pi}^2))$  samples to certify a non-trivially positive lower bound, matching CPI-RR's rate in Theorem 1. This shows the  $1/p_{\pi}^2$  factor is fundamental to CPI-RR

	state $x_1 \in \mathcal{G}_{h,\tau}$ (prob. $p_\pi$ )	state $x_2 \in \mathcal{G}_{h,\tau}^c$ (prob. $1 - p_\pi$ )
action $y_0$	$R_{\max}/2$	$R_{\max}/2$
action $y_1$	$R_{\max}/2 + \tau$	$R_{\max}/2 + \varepsilon$
$y_k, k \geq 2$	$R_{\max}/2$	$R_{\max}/2$

**Figure 5** Reward structure of the  $H = 1$  MDP used in Proposition 10. The base policy plays  $y_0$  everywhere, so  $A^\pi(x, y_0) = 0$ . Only action  $y_1$  on  $\mathcal{G}_{h,\tau}$  (maroon shading) carries the  $\tau$ -advantage signal; all other cells contribute either the baseline (zero advantage) or a negligible  $\varepsilon \ll \tau p_\pi / (1 - p_\pi)$ .

under empirical-mean estimation with only  $\tau, p_\pi$  information — the credit-assignment oracle removes a  $p_\pi^2$  factor that this estimator provably cannot.

The argument is finite-sample anti-concentration for empirical means, in the spirit of Cramer’s theorem for sums of bounded random variables (Dembo and Zeitouni, 2010), made explicit via Berry-Esseen (Lemma 9). We work at  $H = 1$  since the  $H^2$  factor is shared by CPI-RR and CPI-CARO, and our goal is to isolate the  $1/p_\pi^2$  separation.

**Lemma 9** (Berry-Esseen inequality, iid case; Shevtsova, 2010, Theorems 1 and 2). *Let  $Y_1, \dots, Y_n$  be iid real-valued random variables with mean  $\mu_Y := \mathbb{E}[Y_i]$ , variance  $\sigma_Y^2 := \text{Var}(Y_i) > 0$ , and finite third absolute moment  $\rho := \mathbb{E}|Y_i - \mu_Y|^3$ . Let  $\bar{Y}_n := \frac{1}{n} \sum_{i=1}^n Y_i$  and let  $\Phi$  denote the standard normal CDF. Then*

$$\sup_{t \in \mathbb{R}} \left| \Pr((\bar{Y}_n - \mu_Y)/(\sigma_Y/\sqrt{n}) \leq t) - \Phi(t) \right| \leq \frac{0.6 \rho}{\sigma_Y^3 \sqrt{n}}.$$

*Construction.* Fix  $|\mathcal{Y}| \geq 2$  and let  $H = 1$ . The state space has two states  $\{x_1, x_2\}$ , with initial distribution  $\mu(x_1) = p_\pi$  and  $\mu(x_2) = 1 - p_\pi$ . The action set is  $\{y_0, y_1, \dots, y_{|\mathcal{Y}|-1}\}$ , and the base policy plays  $\pi(y_0 | x) = 1$  for all  $x$ . Fix  $\tau \leq R_{\max}/2$  and  $\varepsilon \ll \tau p_\pi / (1 - p_\pi)$ . Rewards have a constant baseline  $R_{\max}/2$  for every action other than  $y_1$ , and a small state-dependent excess for  $y_1$ :

$$r(x, y_k) = R_{\max}/2 \text{ for } k \neq 1, \forall x, \quad r(x_1, y_1) = R_{\max}/2 + \tau, \quad r(x_2, y_1) = R_{\max}/2 + \varepsilon.$$

All rewards lie in  $[0, R_{\max}]$ .

*Resulting structure.* Under  $\pi \equiv y_0$ ,  $V^\pi(x) = R_{\max}/2$  for both  $x$ , and the advantages are  $A^\pi(x_1, y_1) = \tau$ ,  $A^\pi(x_2, y_1) = \varepsilon$ , and  $A^\pi(x, y_k) = 0$  for  $k \neq 1$ . At threshold  $\tau$ ,  $\mathcal{G}_{h,\tau} = \{x_1\}$  with on-policy probability  $p_\pi$ , and the greedy policy  $\pi^+$  plays  $y_1$  everywhere. The expected advantage of  $\pi^+$  against  $\pi$  is therefore

$$\mathbb{A}_{\pi,\mu}(\pi^+) = p_\pi \tau + (1 - p_\pi) \varepsilon = \Theta(\tau p_\pi).$$

**Proposition 10** (Tightness of the random-reset estimator). *Consider the  $H = 1$  construction above with greedy policy  $\pi^+ \equiv y_1$ . Let  $(x_i, y_i)_{i=1}^n$  be iid samples with  $x_i \sim \mu$  and  $y_i \sim \text{Unif}(\mathcal{Y})$ , and define*

$$\hat{\mathbb{A}} := \frac{1}{n} \sum_{i=1}^n Y_i, \quad Y_i := |\mathcal{Y}|(\pi^+(y_i | x_i) - \pi(y_i | x_i)) r(x_i, y_i), \quad \sigma^2 := \text{Var}(Y_i).$$

*Then  $\mathbb{E}[\hat{\mathbb{A}}] = \mathbb{A}_{\pi,\mu}(\pi^+) = \Theta(\tau p_\pi)$  and  $\sigma^2 = \Theta(|\mathcal{Y}| R_{\max}^2)$ . There exist absolute constants  $c_1 > 0$  and  $C_3 \geq 1$  such that, for every sample size  $n$  satisfying*

$$C_3 |\mathcal{Y}|^2 \leq n \leq c_1 \frac{|\mathcal{Y}| R_{\max}^2}{\tau^2 p_\pi^2},$$

$$\Pr(\hat{\mathbb{A}} \leq 0) \geq 0.18.$$

*On the event  $\{\hat{\mathbb{A}} \leq 0\}$ , the CPI-RR step-size formula  $\hat{\alpha} = \min\{1, \hat{\mathbb{A}}/(H^2 R_{\max})\}$  does not produce a valid mixture coefficient, as it returns a non-positive value.*

*Proof.* For the random sampler, each sample  $(x_i, y_i)$  is drawn independently with  $x_i \sim \mu$  (the initial distribution) and  $y_i \sim \text{Unif}(\mathcal{Y})$ . Since  $H = 1$  and rewards are deterministic,  $Q^\pi(x_i, y_i) = r(x_i, y_i)$ . The empirical advantage estimator is

$$\hat{\mathbb{A}} = \frac{1}{n} \sum_{i=1}^n Y_i, \quad Y_i = |\mathcal{Y}|(\pi^+(y_i | x_i) - \pi(y_i | x_i)) r(x_i, y_i).$$

With  $\pi^+ \equiv y_1$  and  $\pi \equiv y_0$ ,  $Y_i$  takes three values, depending on which action  $y_i$  draws:

$$Y_i = \begin{cases} -|\mathcal{Y}| R_{\max}/2 & y_i = y_0, \\ +|\mathcal{Y}| (R_{\max}/2 + A^\pi(x_i, y_1)) & y_i = y_1, \\ 0 & y_i \in \{y_2, \dots, y_{|\mathcal{Y}|-1}\}, \end{cases}$$

where  $A^\pi(x_i, y_1) = \tau$  if  $x_i = x_1$  and  $\varepsilon$  if  $x_i = x_2$ , as defined in the resulting structure above.

*Moments.* Conditional on  $x_i$ ,

$$\mathbb{E}[Y_i | x_i] = A^\pi(x_i, y_1), \quad \mathbb{E}[Y_i^2 | x_i] = |\mathcal{Y}| (R_{\max}/2)^2 + |\mathcal{Y}| (R_{\max}/2 + A^\pi(x_i, y_1))^2.$$

Averaging over  $x_i \sim \mu$  and using  $0 \leq A^\pi(x_i, y_1) \leq \tau \leq R_{\max}/2$ ,

$$\mathbb{A}_{\pi, \mu}(\pi^+) = p_\pi \tau + (1 - p_\pi) \varepsilon = \Theta(\tau p_\pi), \quad \sigma^2 = \Theta(|\mathcal{Y}| R_{\max}^2),$$

with  $\sigma^2 \geq |\mathcal{Y}| R_{\max}^2/4$  (after absorbing  $\tau^2 \leq R_{\max}^2/4$  into the constant).

*Anti-concentration (Berry-Esseen).* Set  $B := 2|\mathcal{Y}| R_{\max}$ . Since  $|Y_i - \mathbb{A}_{\pi, \mu}(\pi^+)| \leq B$ , the third absolute moment satisfies  $\rho = \mathbb{E}|Y_i - \mathbb{A}_{\pi, \mu}(\pi^+)|^3 \leq B^2 \sigma$ . Applying Lemma 9 to  $\{Y_i\}_{i=1}^n$ ,

$$\sup_t \left| \Pr\left(\frac{\hat{\mathbb{A}} - \mathbb{A}_{\pi, \mu}(\pi^+)}{(\sigma/\sqrt{n})} \leq t\right) - \Phi(t) \right| \leq \frac{0.6 \rho}{\sigma^3 \sqrt{n}} \leq \frac{0.6 B^2}{\sigma^2 \sqrt{n}} = \frac{2.4 |\mathcal{Y}|^2 R_{\max}^2}{\sigma^2 \sqrt{n}} \leq \frac{10 |\mathcal{Y}|}{\sqrt{n}} \leq \frac{1}{8}$$

for  $n \geq C_3 |\mathcal{Y}|^2$ , with  $C_3 = 80^2$ . The Berry-Esseen bound then yields anti-concentration via the lower-tail estimate of  $\Phi$ : in the regime  $C_3 |\mathcal{Y}|^2 \leq n \leq \sigma^2/(4 \mathbb{A}_{\pi, \mu}(\pi^+)^2)$ , the rescaled threshold  $\mathbb{A}_{\pi, \mu}(\pi^+) \sqrt{n}/\sigma \leq 1/2$ , so

$$\Pr(\hat{\mathbb{A}} \leq 0) \geq \Phi(-1/2) - \frac{1}{8} \geq 0.18.$$

Substituting  $\mathbb{A}_{\pi, \mu}(\pi^+) = \Theta(\tau p_\pi)$  and  $\sigma^2 = \Theta(|\mathcal{Y}| R_{\max}^2)$ , the regime  $n \leq \sigma^2/(4 \mathbb{A}_{\pi, \mu}(\pi^+)^2)$  takes the explicit form  $n \leq c_1 |\mathcal{Y}| R_{\max}^2/(\tau^2 p_\pi^2)$  stated in the proposition.  $\square$

The lower bound matches the  $1/p_\pi^2$  factor of Theorem 1's upper bound for CPI-RR, so the credit oracle's  $1/p_\pi^2$  saving in Theorem 1 is a genuine algorithmic improvement, not an artifact of loose analysis.

*Interpretation.* The credit-assignment oracle eliminates the  $p_\pi^2$  factor from the sample count *and* amplifies the per-iteration improvement from  $\tau^2 p_\pi^2$  to  $\tau^2 p_\pi$ . Both gains arise from two distinct mechanisms: (1) the larger signal estimated on  $\mathcal{G}_{h, \tau}$ , formalized in the signal-to-noise reading above, and (2) the credit-aware simulation lemma 3, which permits a  $1/p_\pi$ -larger step size in Corollary 5.

## B Implementing the Credit Sampler via Rejection Sampling

Algorithm 3 formalizes the rejection sampler that implements  $\text{CREDIT SAMPLER}(\pi, \mu)$  from the credit-assignment oracle  $\mathcal{O}$ .

---

**Algorithm 3** Rejection-sampling implementation of CREDIT\_SAMPLER( $\pi, \mu$ )

---

**Require:** policy  $\pi$ , initial distribution  $\mu$ , oracle  $\mathcal{O}$ , target count  $n$

- 1:  $\mathcal{D} \leftarrow \emptyset$
  - 2: **while**  $|\mathcal{D}| < n$  **do**
  - 3:     sample  $h \sim \text{Unif}[H]$  and  $x \sim d_\pi^h$  via one reset into  $\pi$ 's trajectory distribution
  - 4:     if  $\mathcal{O}(x, h) = 1$  then  $\mathcal{D} \leftarrow \mathcal{D} \cup \{(x, h)\}$
  - 5: **end while**
  - 6: **return**  $\mathcal{D}$
- 

*Correctness.* Each  $(x, h)$  drawn in line 3 is on-policy; conditioning on the accept event  $\mathcal{O}(x, h) = 1$  returns a sample from the on-policy distribution restricted to  $\mathcal{G}_{h, \tau}$ . The accepted samples are therefore i.i.d. from the target distribution of CREDIT\_SAMPLER( $\pi, \mu$ ).

*Cost.* Each trial succeeds with probability  $p_\pi$ , so  $n$  accepted samples require  $n/p_\pi$  trials in expectation. A trial consists of one reset plus one oracle query, both cheap. Expensive Q-rollouts (Phase 1 of Algorithm 1) are executed only on accepted samples, and thus incur cost  $O(n)$ :

$$\begin{aligned} \text{Cheap calls (reset + oracle query):} & \quad O(n/p_\pi) \\ \text{Q-rollouts:} & \quad O(n) \end{aligned}$$

The Q-rollout count is independent of  $p_\pi$ ; only the rejection step scales as  $1/p_\pi$ .

## C Training Details

*LoRA fine-tuning.* All methods in the main results are trained with LoRA adapters (Hu et al., 2021) (rank 64,  $\alpha = 64$ ); only the adapter parameters are updated, leaving the base model frozen.

*No clipped surrogate.* We do not use the PPO-style clipped surrogate that standard GRPO inherits; we find suffix gradient concentration (from group-relative normalization with prefix masking) sufficiently stable to drive learning without it. Table 4 compares SRPO with and without the clipped surrogate on both base models: clipping does not help on average and underperforms on 14/20 benchmark cells (winning only 4/20, with 2 ties).

**Table 4** Clipped-surrogate ablation: SRPO trained on NuminaMath-Olympiads, with and without the PPO-style clipped ratio. Per-token loss aggregation is suffix-mean  $\rightarrow$  batch-mean in both rows; the only difference is the clip. Single seed (s42), no SD.

Method	oly	hmmt	lvl5	stra	ace	chem	bio	csqa	mat	phys
<i>Qwen2.5-14B-Instruct</i>										
SRPO w/o clip	24.4	10.0	<b>54.6</b>	<b>75.0</b>	45.8	<b>29.2</b>	<b>37.0</b>	<b>79.4</b>	<b>43.0</b>	<b>59.8</b>
SRPO w/ clip	<b>26.2</b>	<b>13.3</b>	53.4	53.0	<b>46.2</b>	24.0	27.0	79.2	28.8	31.4
<i>OLMo-3-7B-Instruct</i>										
SRPO w/o clip	<b>25.0</b>	<b>16.7</b>	<b>68.2</b>	<b>69.6</b>	<b>60.2</b>	<b>22.8</b>	28.4	<b>73.4</b>	<b>55.0</b>	<b>52.0</b>
SRPO w/ clip	<b>25.0</b>	13.3	66.2	66.6	58.8	<b>22.8</b>	<b>32.8</b>	70.8	46.4	48.4

*Hyperparameters.* Table 5 lists the optimization, rollout, loss, and SRPO/RRPO localization settings used across all main results. Values are taken from the trainer log dumps and the launcher (batch\_scripts/submit\_cpio2.sh); we use the same values for both base models, with parallelism scaled to model size.

**Table 5** Training hyperparameters. Identical across base models unless noted.

<i>Optimization</i>	
Optimizer	AdamW
Learning rate	$5 \times 10^{-5}$ (constant)
LR warmup	none
Adam ( $\beta_1, \beta_2$ )	(0.9, 0.999)
Weight decay	0.01
Gradient clipping ( $\ell_2$ )	1.0
LoRA rank / $\alpha$	64 / 64
<i>Schedule</i>	
Epochs	2
Train batch size (prompts)	32
PPO mini-batch size	8
PPO epochs per step	1
Seeds	{0, 42, 420}
<i>Rollout / sampling</i>	
Rollouts per prompt $G$	8
Temperature	0.7
Top- $p$	0.95
Top- $k$	off
Max prompt length	2048
Max response length	4096
Max thoughts per chain	20
Max tokens per thought	256
<i>Hardware / parallelism</i>	
Qwen2.5-14B-Instruct	4 × A100 40 GB, TP= 4
OLMo-3-7B-Instruct	2 × A100 40 GB, TP= 2
Rollout backend	vLLM
Trainer parallelism	FSDP

## D Prompts

*Thought-MDP rollout prompt.* The base agent loop wraps each problem with the template below before sampling thoughts step-by-step. Each thought is generated as a separate vLLM call with stop token `</thought>`; sampling continues until the model emits `\boxed{answer}` or hits the chain cap.

### Thought-MDP rollout

You are solving a problem by producing one reasoning step at a time.  
 Do not try to solve the entire problem at once. Given the previously taken steps, think about what the single next step should be, then articulate it clearly and conclude just that step with `</thought>`.  
 Each step should be a complete, self-contained thought – one observation, calculation, or deduction that: - Makes forward progress toward the solution - Contains substantive reasoning (not filler like "let me think" or restating the problem) - Coheres logically with the previous steps  
 When your next step arrives at the final answer, include `\boxed{answer}` and end with `</thought>`.  
 Q: question

*L2 self-localization prompt.* After a failed Group 1 rollout, the trained policy is queried with the prompt below to identify the originating error step. The chain is rendered as `Step 1: ... / Step 2: ... / ...` with `</thought>` delimiters stripped. Picks come back as `\boxed{N}` and 98% of OLMo-3-7B responses are exactly that token sequence (Section H).

### L2 self-localization

You are tasked with localizing the first erroneous thought in your previous solution to this problem.  
 Problem: question  
 Your incorrect reasoning chain: Step 1: ... Step 2: ... ..  
 The final answer this chain produces is incorrect – therefore at least one step contains an error. The error you are looking for is the originating step where a key decision or action derailed the reasoning, not just the step where the failure ultimately becomes visible. A misread of the problem, an unjustified assumption, or a logical flaw can look fine for several follow-on steps before it surfaces in the wrong answer. A step is erroneous if you cannot justify its claims from the problem statement and earlier verified steps alone. Find the originating step, not just the symptom.  
 Do NOT re-solve the problem. Your ONLY task is to identify the step number of that originating error.  
 Requirements: - Commit to exactly ONE step number (1 to  $n_{steps}$ ). - Stop at the first step you cannot justify. - MANDATORY final line: your response MUST end with `\boxed{N}` on its own line, where N is the step index (1-indexed) of the first erroneous step in the chain above – NOT the answer to the problem. Do NOT add any text after the `\boxed{N}`.

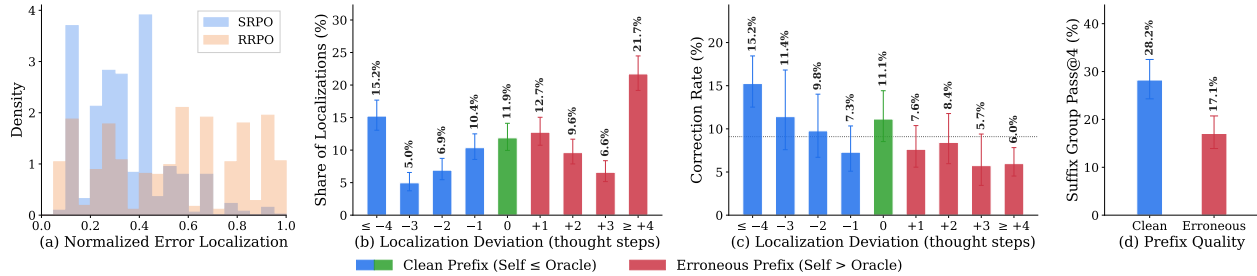


**Figure 6** Self-localization quality on LiveCodeBench v6 (medium), using the raw step-index deviation between SRPO’s self-localization and the Opus oracle. Panels match Figure 4 but without the meaningful-step filter.

## E Self-Localization Quality: Raw Deviation

Figure 6 reproduces the four-panel self-localization analysis from Section 5.3 using the *raw* step-index deviation between the model’s self-localization and the Opus oracle, without any meaningful-step filtering. The eff5 version in the main text (Figure 4) collapses scaffolding steps with fewer than 5 content tokens; the trends in (b)–(d) are qualitatively the same under both definitions.

## F Full Sampling-Strategy Ablation

Table 6 reports the full sampling-strategy comparison from Section 5.1 across both Qwen2.5-14B-Instruct and OLMo-3-7B-Instruct base models. The 1×4 split wins on the majority of columns under both base models.

**Table 6** Sampling-strategy comparison for SRPO under a fixed 8-rollout-per-prompt budget across both base models.

Method	oly	hmmt	lvl5	stra	ace	chem	bio	csqa	mat	phys
<i>Qwen2.5-14B-Instruct</i>										
SRPO (1×4)	25.5 ± 1.2	<b>6.7 ± 2.7</b>	<b>55.2 ± 0.7</b>	<b>74.9 ± 0.2</b>	<b>46.2 ± 0.9</b>	24.5 ± 3.8	<b>33.9 ± 2.3</b>	<b>80.6 ± 0.9</b>	<b>39.3 ± 2.6</b>	<b>45.5 ± 11.8</b>
SRPO (2×4)	<b>25.7 ± 2.0</b>	5.6 ± 1.6	53.4 ± 2.0	60.4 ± 9.3	42.0 ± 0.9	<b>26.0 ± 5.7</b>	32.7 ± 2.8	75.0 ± 1.4	34.3 ± 7.4	34.3 ± 15.6
SRPO (1×8)	25.0 ± 4.8	4.4 ± 1.6	44.4 ± 13.8	71.6 ± 3.3	37.1 ± 9.9	21.2 ± 3.4	32.3 ± 4.0	73.5 ± 5.7	26.6 ± 4.6	27.4 ± 6.5
<i>OLMo-3-7B-Instruct</i>										
SRPO (1×4)	24.8 ± 1.9	<b>15.6 ± 4.2</b>	<b>67.5 ± 3.5</b>	<b>66.6 ± 2.5</b>	<b>59.6 ± 2.6</b>	<b>24.7 ± 1.4</b>	28.7 ± 0.6	<b>74.8 ± 1.0</b>	<b>55.9 ± 0.6</b>	<b>54.5 ± 2.0</b>
SRPO (2×4)	<b>26.1 ± 1.2</b>	14.4 ± 3.1	66.0 ± 3.1	65.9 ± 2.2	56.7 ± 2.7	22.4 ± 0.5	27.9 ± 0.2	65.9 ± 3.3	45.7 ± 1.3	43.2 ± 5.7
SRPO (1×8)	23.1 ± 2.6	12.2 ± 3.1	62.3 ± 2.5	64.1 ± 3.4	53.7 ± 6.3	22.8 ± 1.2	<b>29.8 ± 1.9</b>	59.5 ± 14.9	43.5 ± 5.8	43.4 ± 8.6

## G Per-Token Gradient Concentration

Figure 3 visualizes one SRPO update on a single prompt: four shared-prefix rollouts on top, four base rollouts on bottom. Each rollout is laid out as a sequence of thought blocks (Section 4.1); gray blocks mark the shared prefix that is masked out of the shared-prefix loss, so no gradient lands on those tokens. This appendix derives the per-token gradient signal  $g_{i,t}$  used in Section 5.3, formalizes the per-thought aggregation that determines each block’s color, and shows how  $g_{i,t}$  folds into the gradient of the full SRPO loss.

*Derivation.* For a shared-prefix rollout  $i$  with suffix tokens  $y_{i,1}, \dots, y_{i,T_i}$  sampled under reset state  $x^*$ , the per-token contribution to the loss from Section 4.3 is

$$L_t = -\frac{\hat{A}_i}{T_i} \log \pi_\theta(y_{i,t} | x^*, y_{i,<t}).$$

Writing the policy as a softmax over the actor’s logits  $z = (z_v)_v$ ,  $\pi_\theta(y_{i,t} | \cdot) = \exp(z_{y_{i,t}}) / \sum_v \exp(z_v)$ , we have

$$\log \pi_\theta(y_{i,t} | \cdot) = z_{y_{i,t}} - \log \sum_v \exp(z_v), \quad \frac{\partial \log \pi_\theta(y_{i,t} | \cdot)}{\partial z_{y_{i,t}}} = 1 - \pi_\theta(y_{i,t} | \cdot).$$

Chaining,

$$\frac{\partial L_t}{\partial z_{y_{i,t}}} = -\frac{\hat{A}_i}{T_i} (1 - \pi_\theta(y_{i,t} | \cdot)),$$

and since  $1 - \pi_\theta(y_{i,t} | \cdot) \in [0, 1)$ , the magnitude is  $g_{i,t} = (|\hat{A}_i|/T_i)(1 - \pi_\theta(y_{i,t} | \cdot))$  as used in Section 5.3. The first factor  $|\hat{A}_i|/T_i$  is constant in  $t$  across the rollout’s active region; the second factor is the source of within-trajectory variation. The base group uses the same expression with the full response as the active region.

*Folding into the full loss.*  $L_t$  is one summand of the shared-prefix loss  $\mathcal{L}_{\text{SP}} = \frac{1}{G} \sum_{i=1}^G \sum_{t=1}^{T_i} L_t$ , and  $\mathcal{L}_{\text{base}}$  has the analogous form over full responses. The logit  $z_{y_{i,t}}$  appears in only one summand, so the corresponding entry of the gradient is

$$\frac{\partial \mathcal{L}_{\text{SP}}}{\partial z_{y_{i,t}}} = \frac{1}{G} \frac{\partial L_t}{\partial z_{y_{i,t}}} = -\frac{1}{G} \cdot \frac{\hat{A}_i}{T_i} (1 - \pi_\theta(y_{i,t} | \cdot)),$$

identical for  $\mathcal{L}_{\text{base}}$  at  $T_i$  equal to the full response length.  $g_{i,t}$  is therefore the magnitude of the  $(i, t)$  entry of  $\nabla_z \mathcal{L}$  that the optimizer applies at this step, up to the global rescaling  $1/G$  shared by all entries; Figure 3 plots these entries directly.

*Per-thought aggregation.* A rollout’s active tokens partition into thoughts (Section 4.1). The color of thought block  $(i, h)$  in Figure 3 is the mean of  $g_{i,t}$  over the thought’s active tokens. Masked thoughts (a shared-prefix rollout’s prefix) have no active tokens and are drawn gray. For each prompt  $p$ , we also summarize  $g_{i,t}$  at the group level by first averaging over each rollout’s active tokens,  $\bar{g}_i = \frac{1}{T_i} \sum_{t=1}^{T_i} g_{i,t}$ , and then over the rollouts in that group with nonzero advantage:

$$\bar{g}_{\text{base}}(p) = \frac{1}{n_{\text{base}}^*(p)} \sum_{i \in \text{base}, |\hat{A}_i| > 0} \bar{g}_i, \quad \bar{g}_{\text{SP}}(p) = \frac{1}{n_{\text{SP}}^*(p)} \sum_{i \in \text{SP}, |\hat{A}_i| > 0} \bar{g}_i.$$

A rollout with  $|\hat{A}_i| = 0$  contributes no gradient and is excluded.

*Effect of the prefix mask.* Because the first factor  $|\hat{A}_i|/T_i$  is constant in  $t$  across a rollout’s active region, it sets the per-rollout floor on  $g_{i,t}$ . For a shared-prefix rollout, the prefix mask shrinks  $T_i$  from the rollout’s full-response length to its suffix length, raising that floor on every active (suffix) token of the rollout. The base loss, with no masking, retains the full  $T_i$  and spreads each rollout’s credit across its entire response. We verify this empirically throughout training in §G.1.

## G.1 Gradient signal concentration throughout training

In this LiveCodeBench training run over 1 epoch, we observe that (i) when both rollout groups produce gradient signal on the same prompt, shared-prefix rollouts receive a higher per-token gradient signal than base rollouts; and (ii) the population of signal-bearing shared-prefix groups grows across training as the model’s self-correction skill improves.

We reproduce the LiveCodeBench-medium ep1 schedule on OLMo-3-7B-Instruct (11 update steps, 32 prompts per step, 8 rollouts per prompt) and report  $\bar{g}_i$  averaged within each group on each prompt, then across prompts at each step.

When both groups produce gradient signal on the same prompt, shared-prefix rollouts receive a higher per-token gradient signal than base rollouts:  $\bar{g}^{\text{SP}}/\bar{g}^{\text{base}} > 1$  at 10 of the 11 training steps, range 0.97–1.76, typical value 1.21 (Figure 7, left). The conditioning isolates the architectural claim of §G: group-relative advantages  $\hat{A}_i = (r_i - \bar{r})/\sigma_r$  collapse to zero whenever all four rollouts in a (prompt, group) pair land at the same verifier outcome, so the subset where each group delivers at least one nonzero-advantage rollout is the population on which masking can act.

Shared-prefix groups produce these dual-signal cases less often than base groups (all-same-outcome rates 65–88% for shared-prefix versus 31–66% for base), which is structural: shared-prefix rollouts continue from a

prefix the model has flagged as incorrect, while base rollouts are fresh iid samples from  $x_0$ , so all-fail is the modal shared-prefix outcome. As the policy’s self-correction skill improves across training, the shared-prefix per-rollout pass rate rises from 3.9% at step 1 to 12.5% at step 11 (Pearson  $r = +0.81$  vs. step; Figure 7, right), reducing the shared-prefix all-same-outcome rate from 87.5% to 65.6%. The fraction of prompts where the architectural concentration acts therefore grows across training.

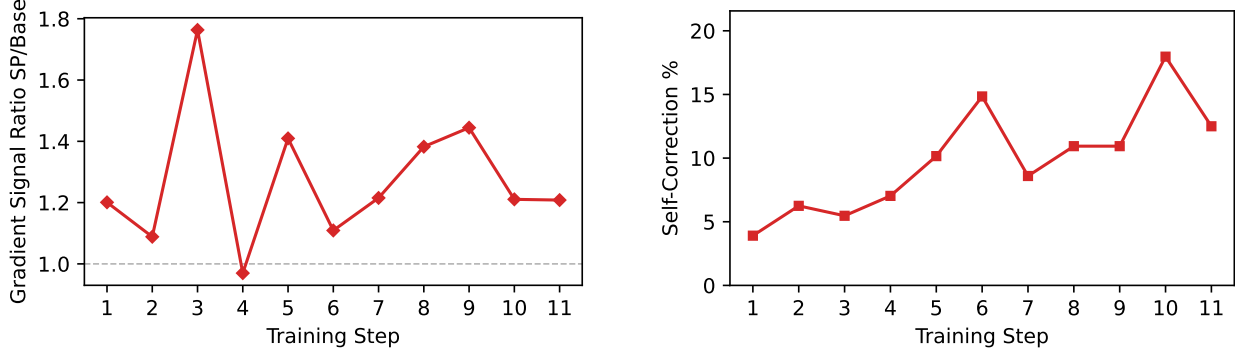


**Figure 7** **Left:** per-token gradient signal ratio  $\bar{g}^{\text{SP}}/\bar{g}^{\text{base}}$  throughout training on prompts where both groups deliver gradient (each group has at least one rollout with  $|\hat{A}| > 0$ ). The ratio exceeds 1 at 10 of 11 steps: the prefix mask is concentrating per-token signal onto the suffix. **Right:** shared-prefix per-rollout pass rate across training (3.9%  $\rightarrow$  12.5%, Pearson  $r = +0.81$  vs. step). As self-correction improves, the shared-prefix group degeneracy rate shrinks from 87.5% to 65.6%, growing the population of prompts on which the left-panel concentration acts. Shared-prefix rollouts are conditional on repairing a flagged-error parent prefix, so this curve measures self-correction specifically.

## H Training Efficiency

We measure per-method compute on LiveCodeBench-Medium with OLMo-3-7B-Instruct (seed 42, one epoch = 11 training steps, 8 rollouts per prompt, batch size 32,  $2 \times$  A100 40 GB per run). Step timings come from the trainer log: `timing_s/step` is the training portion of a step (generation, advantages, log probabilities, actor update); `timing_s/gen` is the generation portion alone; `timing_s/testing` is the validation pass at each step and is method-independent. Total wall clock through ep1 is the sum of `timing_s/step` and `timing_s/testing` over steps 1–11. Table 7 reports raw values; Table 8 normalizes to GRPO.

**Table 7** Per-method compute on lcbm through ep1 (OLMo-3-7B-Instruct, seed 42, 11 steps,  $2 \times$  A100 40 GB). *train\_h* is training-only wall clock; *gen\_h* is rollout generation alone; *val\_h* is the (method-independent) validation pass time; *total\_h* = *train\_h* + *val\_h*; *tokens* is  $\sum \text{perf}/\text{total\_num\_tokens}$  (all forward-passed tokens in training steps); *resp $_{\mu}$*  is mean response length across rollouts; *gen tok/s* is *tokens/gen\_h*.

Method	train_h	gen_h	val_h	total_h	tokens	resp $_{\mu}$	gen tok/s
GRPO	3.44	2.70	4.32	7.75	8.10 M	2281	833
RRPO	5.33	4.48	6.50	11.83	9.94 M	2932	617
SRPO	5.21	4.36	4.93	10.14	8.75 M	2510	557

**Table 8** Same quantities normalized to GRPO (= 1.00).

Method	train	gen	total	tokens	resp $_{\mu}$
GRPO	1.00	1.00	1.00	1.00	1.00
RRPO	1.55	1.66	1.53	1.23	1.29
SRPO	1.51	1.61	1.31	1.08	1.10

*Discussion.* SRPO emits  $1.08 \times$  as many tokens as GRPO through ep1, and RRPO  $1.23 \times$ , despite both running a second group of  $G$  rollouts on top of the base group:  $G_2$  shares the  $G_1$  prefix up to the reset step, so only the suffix is autoregressively sampled rather than a full fresh rollout (mean suffix length  $\approx 1720$  tokens

for SRPO at step 1). Training-only wall clock is  $\sim 1.5\times$  GRPO (Table 8), reflecting the serial dependency of G2 on the self-localization step computed from G1.

*Localization-call cost.* The token counts above include only G1+G2 rollout tokens; the self-localization call’s output is discarded as non-training data and is not in `perf/total_num_tokens`. For OLMo-3-7B-Instruct on lcbm, this omission is negligible: 98% of localization responses are just `\boxed{N}<|endoftext|>` ( $\approx 9$  tokens), totalling  $\sim 3$  K tokens across the entire ep1 (0.04% of training tokens). Models with more verbose localization behavior could push this share materially higher, so future runs should log per-call localization output length and add it to the token total.